HF Radar Observations of Inter-Annual variations in Mid-Latitude Mesospheric Winds

Garima Malhotra

Dissertation submitted to the Faculty of the
Virginia Polytechnic Institute and State University
in partial fulfillment of the requirements for the degree of

Masters in Science
in
Electrical Engineering

Joseph B. Baker, Co-Chair
J. Michael Ruohoniemi, Co-Chair
Wayne A. Scales
Robert C. Clauer

April 9, 2016
Blacksburg, Virginia

Keywords: Mid-Latitude QBO, Mesospheric QBO, Holton Tan, Gravity wave filtering, SuperDARN radar, SuperDARN Radar Mesospheric winds, HF Radar Meteor echoes

HF Radar Observations of Inter-Annual variations in Mid-Latitude Mesospheric Winds

Garima Malhotra

(ABSTRACT)

The equatorial Quasi Biennial Oscillation (QBO) is known to be an important source of inter-annual variability at mid and high latitudes in both hemispheres. Coupling between QBO and the polar vortex has been extensively studied over the past few decades, however, less is known about QBO influences in the mid-latitude mesosphere. One reason for this is the relative lack of instrumentation available to study mesospheric dynamics at mid-latitudes. In this study, we have used the mid-latitude SuperDARN HF radar at Saskatoon (52.16°N, -106.53°E) to study inter-annual variation in mesospheric winds. The specific aim was to determine whether or not a Quasi Biennial signature could be identified in the Saskatoon mesosphere, and if so, to understand its relationship with the equatorial stratospheric QBO. To achieve this goal, a technique has been developed which extracts meteor echoes from SuperDARN near-range gates and then applies least-squares fitting across all radar beam directions to calculate hourly averages of the zonal and meridional components of the mesospheric neutral wind. Subsequent analysis of 13 years (2002-2014) of zonal wind data produced using this technique indicates that there is indeed a significant QBO signature present in Saskatoon mesospheric winds during late winter (Jan-Feb). This mesospheric QBO signature is in opposite phase with the equatorial stratospheric QBO, such that when QBO (at 50 hPa) is in its easterly (westerly) phase, the late winter winds in Saskatoon mesosphere become more (less) westerly. To further examine the source of the signature, we also analyzed winds in the Saskatoon stratosphere between 5 hPa and 70 hPa using the ECMWF ERA-Interim reanalysis data set, and found that the late winter stratospheric winds become less (more) westerly when QBO is easterly (westerly). This QBO signature in the mid-latitude stratospheric winds is essentially the same as that observed for the polar vortex in previous studies but it is opposite in phase to the mid-latitude mesospheric QBO. We therefore conclude that filtering of gravity waves through QBO-modulated stratospheric winds plays a major role in generating the mesospheric QBO signature we have identified

in the Saskatoon HF radar data. When the Saskatoon stratospheric winds are anomalously westward during easterly QBO, the gravity waves having westward momentum might be filtered out, depositing a net eastward momentum in the mesosphere as they propagate upwards. This would result in increased westerly mesospheric winds at Saskatoon. The opposite would happen when the equatorial QBO is westerly.

This work was supported by National Science Foundation grants AGS-1341918 and AGS-1150789.

Acknowledgments

I would like to start by thanking my advisors Jo and Mike. Words are less to describe how grateful I am to both of you for trusting me and guiding me in the best way possible throughout my time in VT SuperDARN. Thank you for giving me this wonderful opportunity to study space physics, being patient with me and providing me the freedom to explore and find my way through. Jo, thank you for your tireless efforts throughout the paper and thesis writing process. I would also like to take this opportunity to thank my co-authors, especially Dr. Robert Hibbins for actively engaging in this work.

This work would not have been possible without the help I received from Nathaniel, in Python, IT and general OS issues. Nathaniel, you have been a great teacher and watching you and your enthusiasm has been very motivating. This work is also dedicated to my friends and labmates in these past few years, Xueling, Pratik, Muhammad, Kevin and Evan. I have my best memories in Space@VT with Xueling because of her great support and help. People like you are hard to find, and I wish to hold onto your friendship for years to come. Thank you Pratik, for telling me all about how amazing working in SuperDARN would be. I still remember waiting to meet Pratik (during my first week at Virginia Tech) outside Space@VT, while he told me that the group meeting will be over in 45 minutes. The meeting ended after 2.5 hours. Monday Group meetings are never 'short and simple' here (as Mike wishes them to be).

I am extremely grateful to my family, especially my parents, Som and Jyoti for giving me the freedom to choose my career path, even though it wasn't easy for them to let me go. My brother, Rohit and my grandparents who have always been extremely supportive of my

academic career, Thank you! Special thanks to all my friends, especially, Vidhi, Rashmi, Aparajita, Nandita, Chaitra, Shekar for always being there. Thank you Anshul, for your constant motivation in these past few years, encouragement and belief in me.

Contents

List of Figures

Chapter 1

Introduction

This chapter aims to introduce the basic dynamics of the Mesosphere and Lower Thermosphere (MLT) region of Earth's atmosphere. We discuss planetary waves, gravity waves and long term variations such as the Quasi Biennial Oscillation (QBO). This work aims to investigate the Quasi Biennial Signature in the mid-latitude mesosphere and its relationship to the Equatorial QBO. Therefore, in this chapter we also introduce the mechanisms that might be involved in coupling latitudinally (via planetary waves) and vertically (via gravity waves) the equatorial stratospheric QBO to the extratropical mesosphere.

1.1 Earth's Atmosphere

The Earth's atmosphere can be classified to different layers depending on the temperature gradient in each region (Figure 1.1). The lowest layer of the Earth's atmosphere is the troposphere where most of weather phenomena take place and the temperature decreases with altitude with a lapse rate of 7 K/km [*Kelley*, 2009]. This trend reverses at the tropopause ($\sim$10 km) above which the stratosphere starts. The stratosphere has the maximum density of ozone and hence absorbs in the ultraviolet portion of the solar spectrum. The temperature increases with altitude until the stratopause ($\sim$50 km). The temperature trend reverses again in the mesosphere and reaches its minimum value (-90°C) at $\sim$ 80-90 km altitude. This

is partially because of high radiative cooling in this region. The mesosphere is also the region where most meteors burn up upon entering the Earth's atmosphere. Above the mesosphere, is the thermosphere, where temperature increases with height due to the absorption of solar high energy ultraviolet and x-ray radiation and other influences. The density decreases in this region and the pressure is very low with few collisions and high average molecular kinetic energies.

The atmosphere is quite uniform in composition below mesospheric heights due to turbulent mixing. Above this, the constituents begin to separate according to their masses. The Mesosphere and Lower Thermosphere (MLT) region (60-110 km) marks the transition between the lower atmosphere which is dominated by turbulent mixing and the upper atmosphere which is dominated by molecular diffusion. The transition boundary is called the turbopause. The height of the turbopause varies and is highly influenced by wave phenomena initiated from below. To understand the vertical coupling between the lower and upper atmosphere, it therefore becomes necessary to understand the dynamics of the MLT region.

1.2 Mesosphere and Lower Thermosphere

The Mesosphere and Lower Thermospheric region is the region between 60-110 km altitude that is characterized by complex dynamics. It is influenced by a number of external sources such as solar UV and EUV radiation, auroral and energetic particle precipitation, magnetospheric plasma convection and wave activity propagating from the lower regions of the atmosphere. This region has been studied widely over the last few decades in numerous modeling studies but its location in the middle atmosphere makes it difficult to obtain reliable data via satellites. Instead, data tends to be provided by medium frequency (MF) radars, meteor radars, incoherent scatter radars (ISR) and rockets.

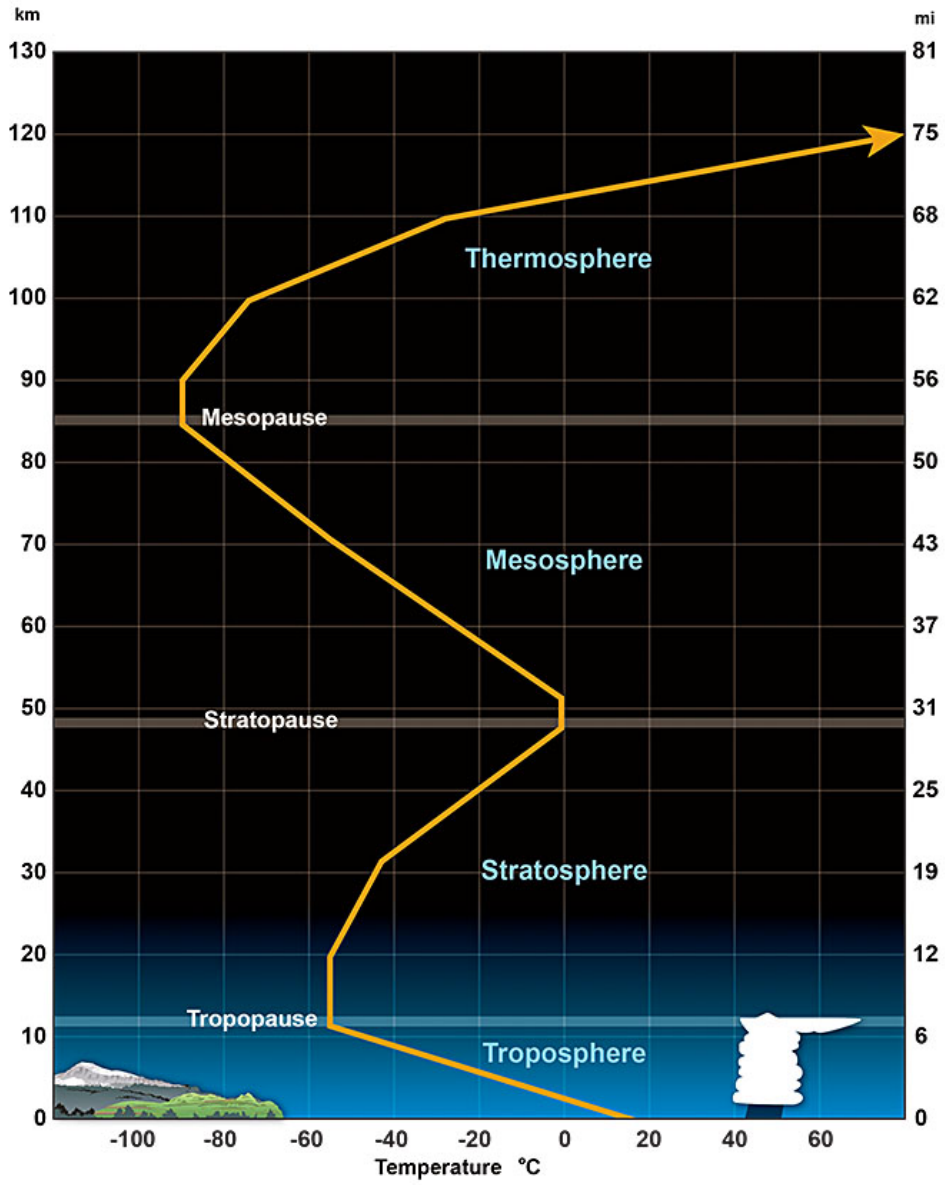

Figure 1.1: An average temperature profile of the Earth's atmosphere. Height (in miles and kilometers) is indicated along vertical axes. The horizontal axis represents temperature in degree Celsius. Source: Jetstream, National Weather Service

1.2.1 Dynamics

The MLT region is highly influenced by the effects of atmospheric waves such as gravity waves, planetary waves and atmospheric tides. These waves grow in amplitude as they rise higher in the atmosphere due to decreasing neutral density [*Andrews et al.*, 1987]. They are either generated in-situ or propagate up from the lower levels and break or dissipate depositing their momentum and energy, thereby mixing atmospheric species and interacting with other waves or the mean flow. These waves can also transport chemically and radiatively active species from other regions of the atmosphere, thus playing a crucial role in the energy budget and dynamics of the MLT. Specifically, these interactions are thought to provide ∼70% of the energy and momentum budget in the MLT [*Johnson and Killeen*, 1995]. Furthermore, the wave forcing takes the MLT region far from its radiative equilibrium.

1.3 Gravity waves

Gravity waves are buoyancy waves that propagate vertically and horizontally away from their source with periods ranging between a few minutes to a few hours, and horizontal wavelengths of tens to thousands of kilometers. Gravity waves are generated in a fluid medium or at the interface between two media when the force of gravity or buoyancy tries to restore equilibrium. When a fluid element is displaced into a region with a different density, gravity will try to restore it toward equilibrium, resulting in an oscillation about the equilibrium state. These oscillations then tend to propagate as gravity waves. They lead to oscillations in wind, density, pressure and temperature and have vertical wavelengths of a few to tens of kilometers.

If we drop a stone in a pool, the ripples that spread outward are gravity waves. Common sources of gravity waves in the atmosphere include topographic features (Figure 1.2), frontal and convective activity and wind shear. Gravity waves can often be seen as billowing patterns of mesospheric noctilucent clouds (Figure 1.3), and shifting bands of airglow. They dissipate and deposit their momentum, driving the circulation in the MLT. Hence, they are crucial

for understanding the dynamics and variabilities in this region.

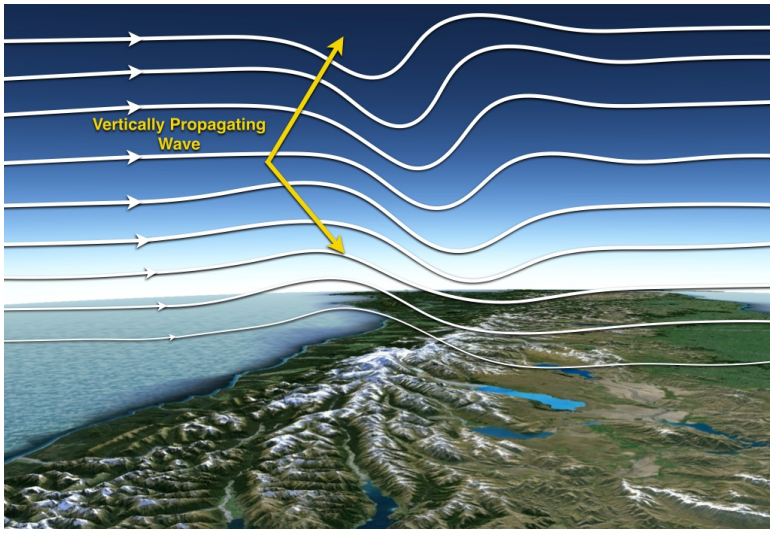

Figure 1.2: Generation of gravity waves on being obstructed by mountain. The wave that is generated then propagates vertically to higher altitudes. One vertical wavelength is shown here.
Source: @UCAR, by Alison Rockwell, NCAR Earth Observing Laboratory.

Figure 1.3: Noctilucent clouds in the polar mesosphere. Gravity wave structures can be observed in the billow patterns.
Source: Leibniz-Institute of Atmospheric Physics.

1.4 Planetary Waves

Planetary waves are long period global oscillations which are either stationary (i.e., fixed to the Earth) or zonally propagating in either direction. Planetary waves are generated by the gradient in the potential vorticity from equator to pole, topographic features, and by gradients in land-sea temperatures.

Their periods range between 2 days to 27 days, and horizontal wavelengths range between 50 to 180 degrees of longitude. The wavenumbers vary from 6 to 2. Figure 1.4 shows a visualization of planetary wave structure in the polar jet stream by NASA/GSFC. Specific to this study, planetary waves play an important role in the circulation of stratospheric winds. This further affects the gravity wave momentum fluxes reaching up into the MLT. Therefore, understanding their dynamics and effects will help us in our investigation of the influences on MLT from the lower atmosphere.

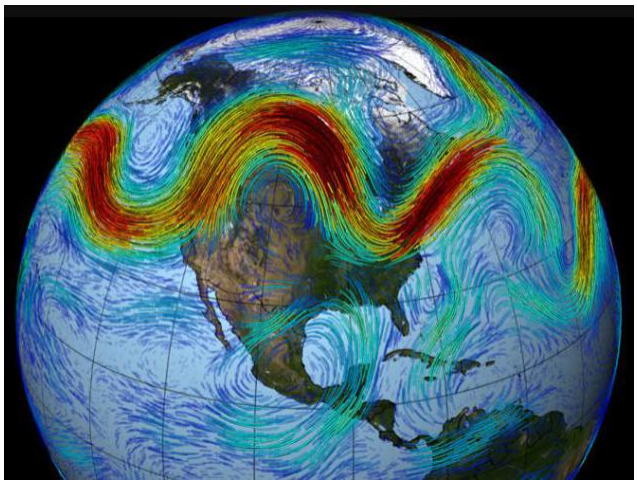

Figure 1.4: A visualization of polar jet stream flowing eastwards across the mid-latitudes of North America. The data is taken from the weather and climate observations from NASA's MERRA dataset.
Source: NASA/GSFC

1.5 Quasi Biennial Oscillation

The MLT is not only dominated by planetary waves and gravity waves but also has strong interannual and long term variations such as the Quasi Biennial Oscillation.

The Quasi Biennial Oscillation (QBO) is an important mode of interannual variability in the equatorial stratosphere which has widespread influences in both hemispheres. It was discovered independently by *Reed et al.* [1961] and *Ebdon* [1960] and is characterized by zonally symmetric alternating regimes of easterly and westerly winds that propagate downward in the equatorial stratosphere with an average cycle of 28-36 months [*Naujokat*, 1986; *Baldwin et al.*, 2001]. Figure 1.5 shows the equatorial zonal winds at Singapore radiosonde station. These bands originate at a height of 30 km and then move downward through the stratosphere with a speed of 1 km/month [*Reed et al.*, 1961]. QBO is generated by an internal two-way feedback mechanism between the vertically propagating gravity waves and the background mean flow. The first part of the feedback is the effect of the background flow on the propagation of gravity waves and the second part is the effect of wave momentum fluxes on the background flow [*Baldwin et al.*, 2001].

1.6 Coupling Mechanisms

Although QBO is a tropical phenomenon, it affects the stratospheric flow from pole to pole by modulating the effects of extratropical waves. Various influences transport the QBO signal from the equator to the extratropical latitudes, including planetary and gravity waves.

1.6.1 Latitudinal Coupling of QBO to Extratropics

Dynamical coupling between the QBO and the high-latitudes, specifically the stratospheric polar vortex in both the hemispheres, has been extensively studied using both observations and models, yet the exact mechanism behind this coupling is not well understood. *Holton and Tan* [1980] demonstrated weaker polar vortex during the easterly phase of QBO (50

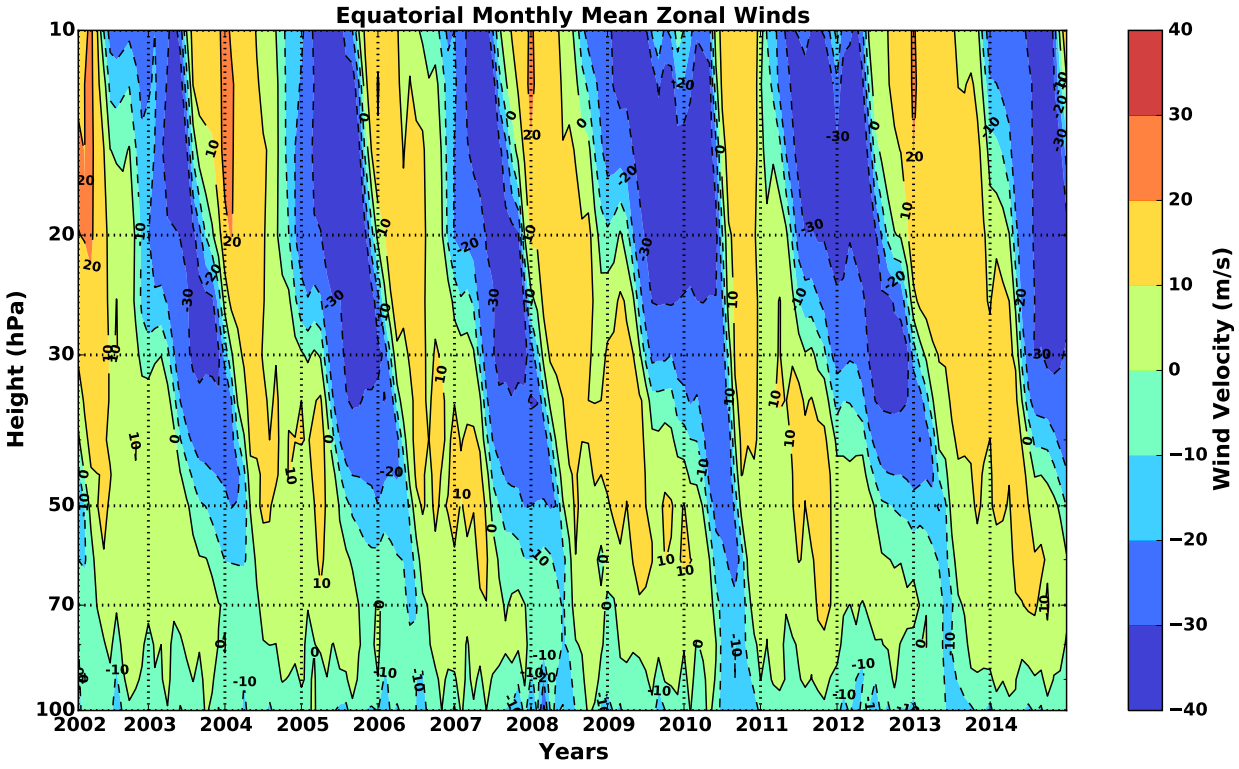

Figure 1.5: Height resolved stratospheric zonal winds at the Singapore equatorial radiosonde station for 2002-2014. The contour interval is 10 m/s with colors representing wind velocities in m/s. Red represents westerly winds, whereas blue represents easterly winds.

hPa) using geopotential height data during northern winter.

The polar vortex is a winter-time phenomenon, essentially described as a large-scale cyclone of eastward blowing cold air in the polar regions. It strengthens in the winter and is located in the middle and upper troposphere extending into the stratosphere. Planetary waves are generated in the troposphere and may propagate into the stratosphere during winter when the zonal-mean zonal wind is westerly. When these waves dissipate in the stratosphere, they decelerate the zonal-mean zonal wind (westerly) away from the radiative equilibrium state of a strong and cold circumpolar vortex.

Holton and Tan [1980] described the QBO-vortex coupling (also known as the Holton-Tan effect) as the influence of planetary waves in the winter hemisphere via modulation of the subtropical zero-wind critical line by the phases of QBO. This line is the critical line for planetary waves beyond which they cannot propagate into the summer hemisphere. When QBO (at 50 hPa) is easterly, the zero wind line moves poleward into the winter subtropics thus latitudinally limiting the winter westerly winds, resulting in focusing of planetary wave activity toward high latitudes. This increased extratropical planetary wave activity will lead to a more disturbed and weaker polar vortex. Whereas when QBO is westerly, the planetary wave activity will be less confined in the winter hemisphere, resulting in a stronger polar vortex [*Anstey and Shepherd*, 2014]. This wind line movement is demonstrated in Figure 1.6. The observations from *Lu et al.* [2008] are shown in Figure 1.7. When QBO at 50 hPa is easterly during winter, polar vortex weakens (dotted contours), whereas when QBO is westerly, the polar vortex strengthens (solid contours).

1.6.2 Vertical Coupling of QBO to Mesosphere

QBO signal is not only observed in the stratosphere, but also extends up into the mesosphere. Equatorial Mesospheric QBO was first studied by *Burrage et al.* [1996] and he found that the phase of the Mesospheric QBO is opposite to the stratospheric QBO. It is believed that some of the gravity waves do not dissipate in the middle atmosphere but reach up into the MLT region and dissipate, generating Mesospheric QBO at the equator. The opposite phase

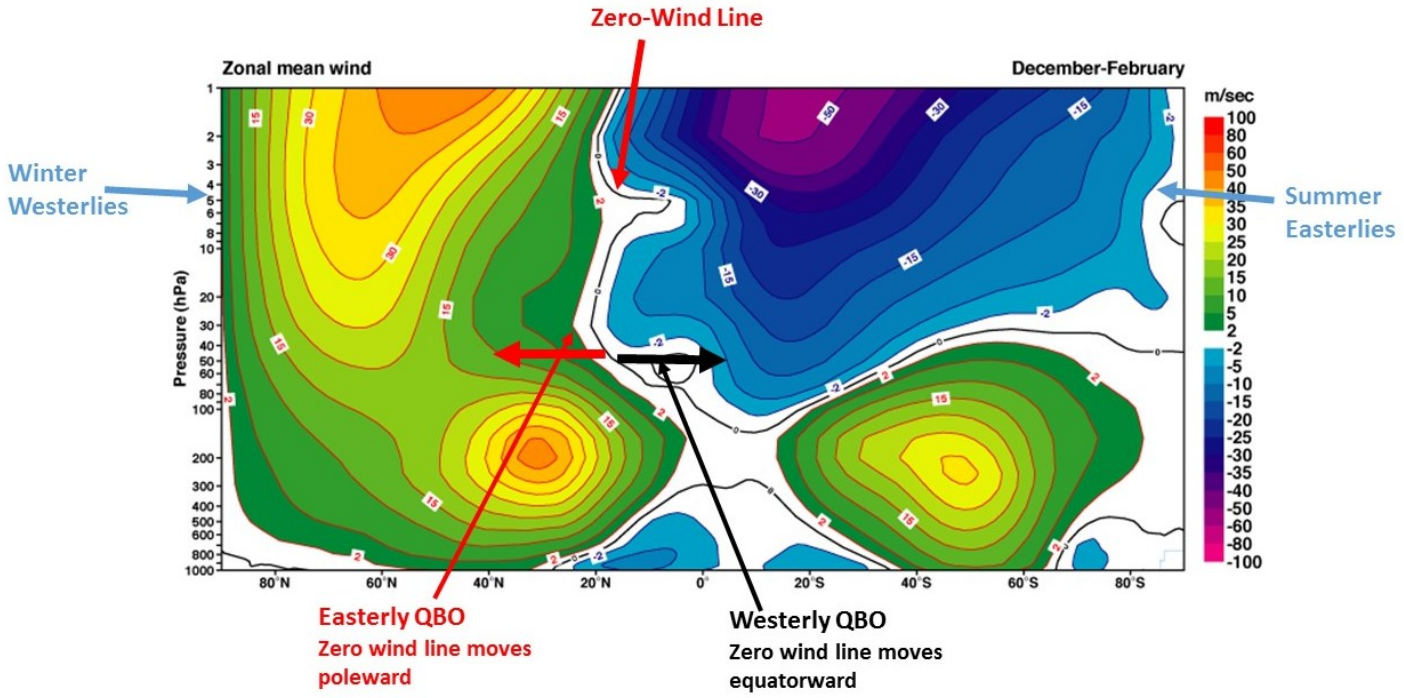

Figure 1.6: Zonal mean zonal wind climatology averaged from December to February. The horizontal axis represents latitude and the vertical axis represents altitude in hPa. The winter hemisphere is dominated by westerly winds, whereas the summer hemisphere is dominated by easterly winds. The movement of the zero-wind line during different phases of QBO is indicated.
Source: Adapted from ECMWF: ERA-40 Atlas

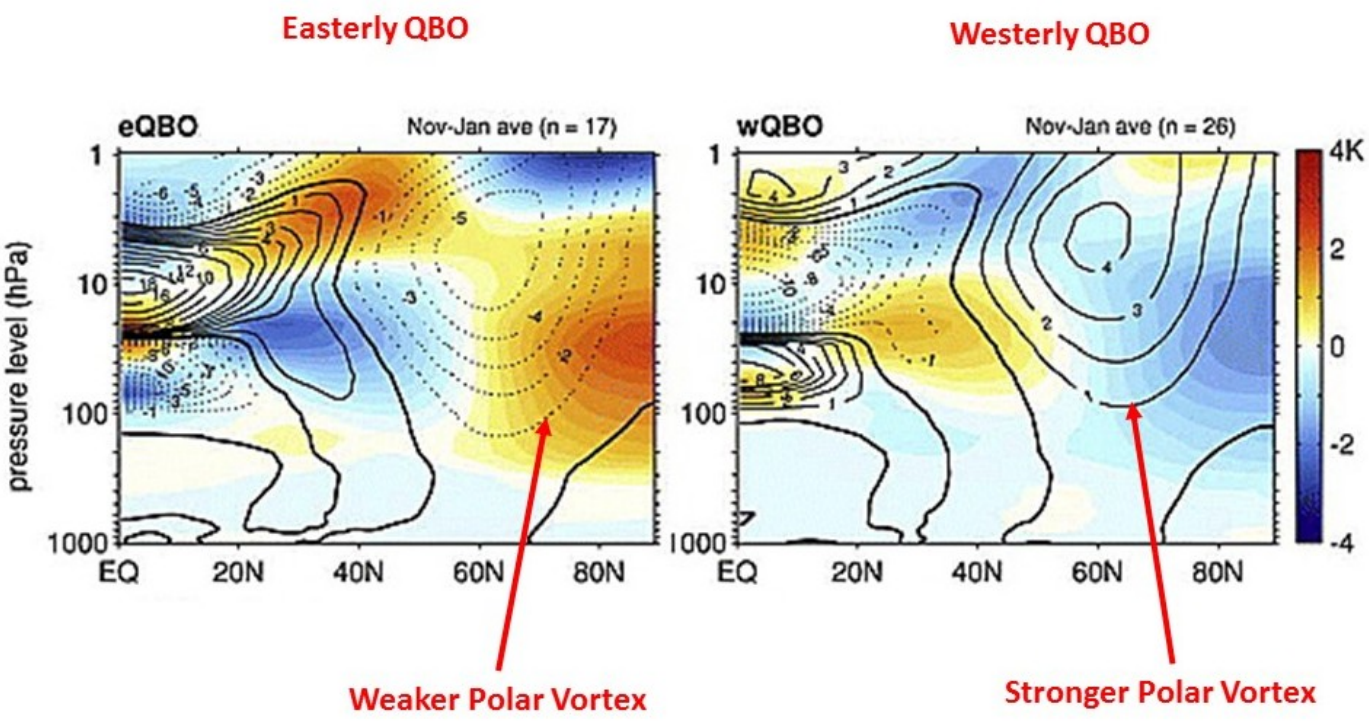

Figure 1.7: QBO-Polar Vortex coupling: e-QBO (left-hand panel) and w-QBO (right-hand panel) composites of the zonal mean zonal wind (lined contours) and temperature anomalies (color shaded contours) for November to January mean. Thick solid lines represent zero wind. The total number of data samples are indicated on the top of each panel.
Source: Adapted from [*Lu et al.*, 2008]

is because of the critical level filtering of the gravity waves by the underlying QBO [*Burrage et al.*, 1996].

A critical level occurs (and the wave is absorbed by the background wind) when the phase velocity of the wave becomes equal to the background wind speed. Thus, the gravity waves encounter their critical levels and are filtered as they propagate through the stratosphere. As these filtered waves reach into the MLT region, their amplitude, energy and momentum increases, resulting in wave breaking, dissipation and momentum deposition (like ocean waves breaking at the beach). The momentum that is then deposited in the MLT is generally opposite to the direction of the stratospheric zonal winds. An example of this can be seen in the gravity wave flux observed in the MLT region during winter and summer. In summer, only eastwards propagating gravity waves with phase speeds greater than the tropospheric and stratospheric maximum mean zonal wind speeds, may enter the mesopause region. In contrast, all westward propagating waves may reach the mesopause region during winter, as the wind profile lower down is westerly. This filtering mechanism is shown in Figure 1.8.

A westerly phase of stratospheric QBO thus produces the gravity wave spectrum with dominant westward momentum, which will eventually dissipate in MLT giving rise to the easterly phase of MQBO. Whereas the easterly phase of stratospheric QBO will produce the gravity wave spectrum with dominant eastward momentum, giving rise to westerly phase of MQBO. Figure 1.9 shows the results presented by *Burrage et al.* [1996] using high resolution Doppler imager (HRDI) on the Upper Atmosphere Research Satellite (UARS). At ∼85 km altitude, the mesospheric QBO opposite in phase with the stratospheric QBO can be observed.

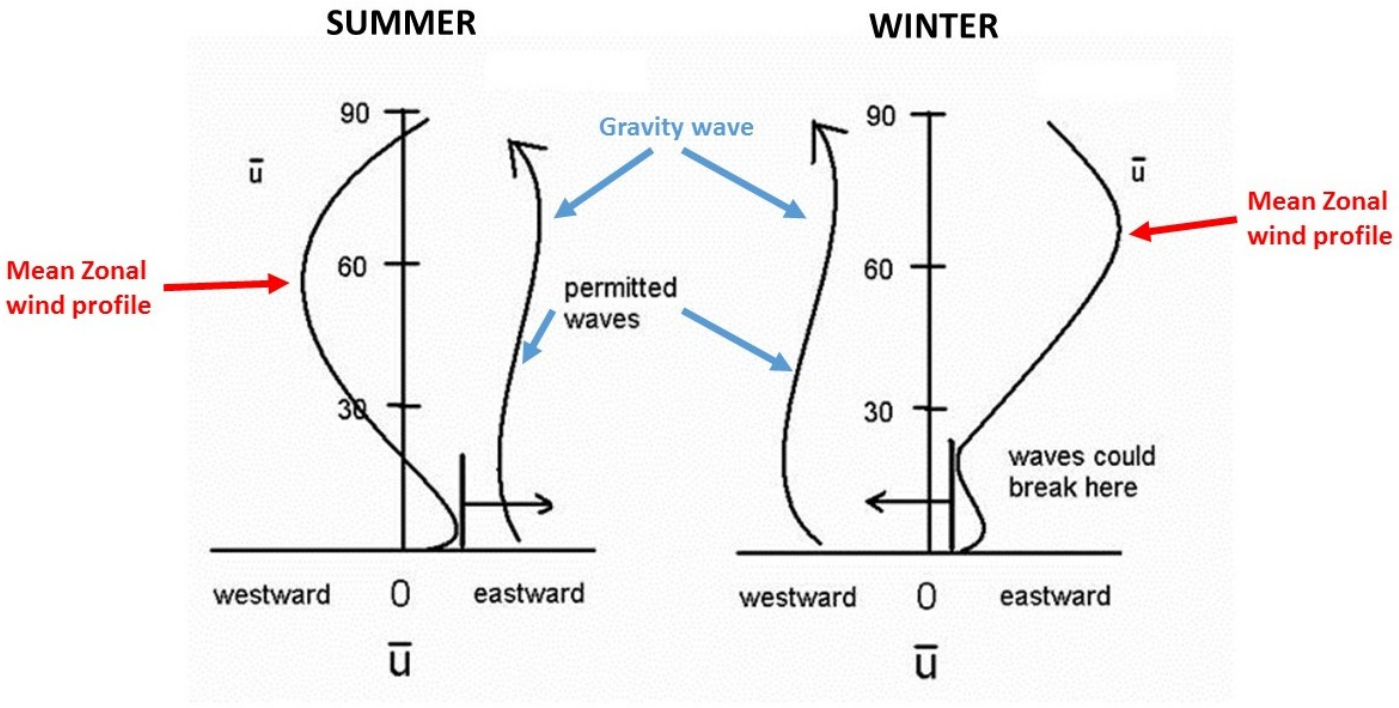

Figure 1.8: A schematic diagram showing the dominating gravity wave flux during summer (left) and winter (right). Vertical axis is indicative of height in the atmosphere, and horizontal axis represents the wind speeds.

Source: Adapted from Meteo 465, Middle Atmospheric Dynamics, Penn State University.

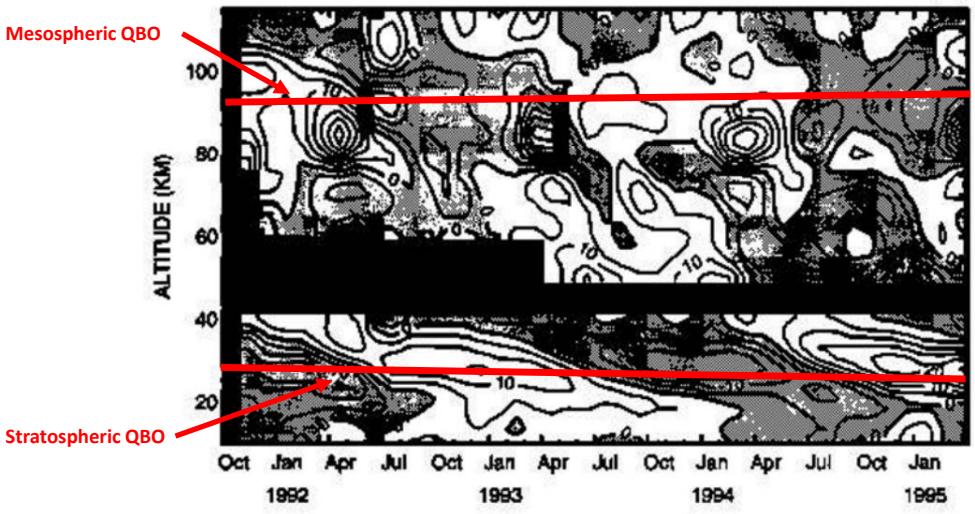

Figure 1.9: Mesospheric QBO as observed by *Burrage et al.* [1996]. Residual zonal wind observed by HRDI as a function of altitude and time at the equator. The residual wind is defined as the mean background wind minus the annual and semiannual components and the linear trend and mean. The contour levels are given every 10 m/s.

1.7 Summary

The current state of knowledge of the mechanism of generation for the equatorial QBO and its dynamic coupling with the equatorial mesosphere and high-latitude stratosphere can be summarised by a schematic diagram by *Baldwin et al.* [2001] shown in Figure 1.10.

Equatorial QBO is generated by the interaction of gravity waves with the mean flow. It is marked by the downward propagating phases of easterly and westerly wind regimes, with a period of 28-36 months. This stratospheric QBO generates an opposite phase signature with a biennial periodicity in the equatorial mesosphere via filtering of gravity waves at critical levels. The QBO also manifests itself at high-latitudes via latitudinal coupling through

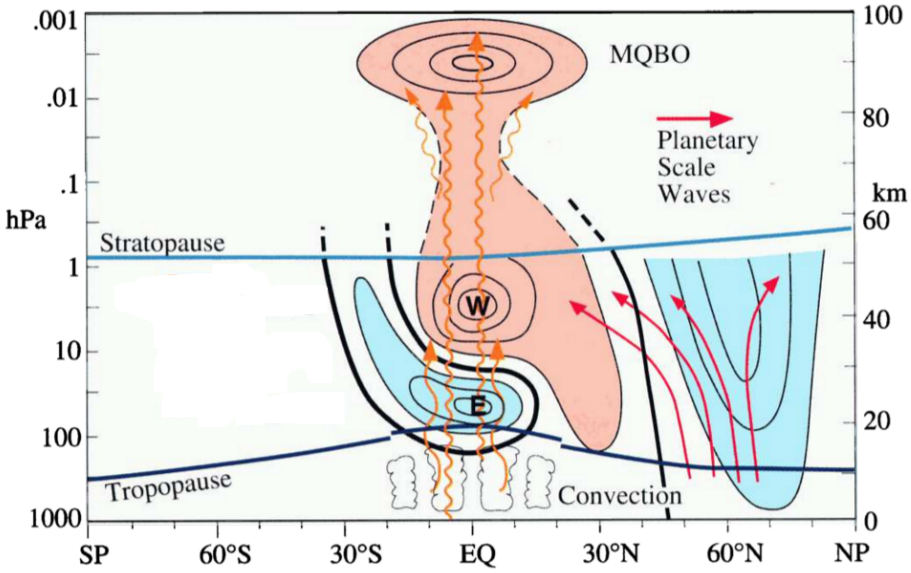

Figure 1.10: (Adapted from *Baldwin et al.* [2001]) Figure demonstrating the generation of QBO and its coupling to the equatorial mesosphere and high-latitude stratosphere during northern winter. The propagation of various tropical waves is depicted by orange arrows, with the QBO driven by upward propagating gravity waves. The propagation of planetary-scale waves (purple arrows) is shown at middle to high latitudes. Black contours indicate the difference in zonal-mean zonal winds between easterly and westerly phases of the QBO, where the QBO phase is defined by the 40-hPa equatorial wind. Easterly anomalies are light blue, and westerly anomalies are pink. In the tropics, the contours are similar to the observed wind values when the QBO is easterly. The mesospheric QBO (MQBO) is shown above ∼80 km, while wind contours between ∼50 and 80 km are dashed due to observational uncertainty.

planetary waves. The coupling of QBO with the polar vortex was explained by *Holton and Tan* [1980]. When QBO is easterly at 50 hPa, the polar vortex weakens due to higher planetary wave activity in the winter hemisphere, whereas when QBO is westerly at 50 hPa, the polar vortex is stronger due to lower planetary wave activity.

1.8 Outstanding Questions and Thesis Objectives

The shifting of the zero-wind line mechanism has been under speculation for several decades due to inconclusive results of planetary wave fluxes in the winter hemisphere [*Holton and Tan*, 1980, 1982; *Dunkerton and Baldwin*, 1991] and several other mechanisms have since been suggested [*Garfinkel et al.*, 2012; *Gray et al.*, 2001a, 2004; *Pascoe et al.*, 2006; *Naoe and Shibata*, 2010] for the observations of Holton-Tan (HT) relationship.

The signature of the QBO in the extratropical mesosphere is also not well understood. At mid-latitudes, the mean zonal wind in the MLT region has been shown to exhibit a QBO signature, however previous studies could not link it to the equatorial stratospheric QBO [*Namboothiri et al.*, 1993, 1994]. At high latitudes, *Baumgaertner et al.* [2005] did not find any QBO effect on mean winds or tides at Scott Base (78°S, 167°E), Antarctica, using MF radar. However, mesospheric QBO signature has been observed in the semidiurnal tides [*Hibbins et al.*, 2007, 2010; *Jarvis*, 1996] and planetary waves [*Hibbins et al.*, 2009].

Thus, there are several outstanding questions regarding the mechanism of interaction between the QBO and extratropical latitudes which still remain to be answered. Specifically, is there a QBO signal present in the mid-latitude mesosphere and stratosphere? And, if so, is there any vertical interaction between the extratropical stratospheric and mesospheric QBO signal?

To date, there has not been a comprehensive investigation of the QBO signature in the mesosphere at mid and high latitudes. This study is a step in that direction. Our objective is to look for a QBO signature in the mid-latitude mesosphere and (if found) understand its relationship to the equatorial QBO and generation mechanism. Meeting the objective will

allow us to better understand how the QBO couples to the extratropics and how it influences the meridional coupling between the winter and summer hemisphere.

Chapter 2

Pre-processing of SuperDARN Wind Data

In this study, we aim to investigate the inter-annual variations, specifically the QBO, in the mid-latitude mesosphere using the SuperDARN radar at Saskatoon (52.16°N, -106.53°E). In Chapter 1, we reviewed the latitudinal and vertical coupling mechanisms involved in transporting the equatorial QBO signature to extratropical latitudes and into the mesosphere. This chapter aims to introduce the basic techniques and principles used in determining the mesospheric neutral winds from the SuperDARN HF meteor backscatter. We first summarise the basic principle of SuperDARN HF radars and meteor backscatter and then discuss the filtering and fitting analysis involved in calculating the wind velocities.

2.1 SuperDARN Radars

The Super Dual Auroral Radar Network (SuperDARN) is an international network of HF radars in the northern and southern hemisphere used to study plasma convection in the E and F region of the ionosphere [*Greenwald et al.*, 1985]. The radars cover a wide region of the auroral, sub-auroral, polar, and mid-latitude ionosphere. Figure 2.1 shows locations of the SuperDARN radars and their field of views in the Northern and the Southern Hemi-

sphere as of March, 2016. These radars employ the refractive properties of the ionosphere to receive backscatter from ionospheric irregularities. As an HF wave propagates through the ionosphere, it refracts, and can be reflected by field aligned plasma irregularities when the angle between the propagation direction and the magnetic field is close to 90°. The radars also receive another type of backscatter (called "Ground Scatter") which is the backscattered radar signal from the ground. Both the ionospheric and ground scatter are used to study a number of ionospheric phenomena. [*Ruohoniemi et al.*, 1987; *Chisham et al.*, 2007]

SuperDARN radars operate within the frequency range of 8-20 MHz and consist of 16 log-periodic or twin-terminated folded dipole (TTFD) antennas (Figure 2.2) which are phased electronically to form a narrow beam (∼3.3°) which can be steered in 16-22 directions covering a range of ±26° from the boresight direction. The peak power is 10 kW and the pulse width of 200-300 microseconds gives a range resolution of 45 km. The radars scan through beam positions remaining in each position for ∼ 3 or 6s typically so that the entire field of view is scanned in 1 or 2 minutes. The first range gate starts at 180 km in range with at least 75 range gates extending to a maxiumum range of ∼3555 km (where each range gate is 45 km long). The radars transmit multipulse sequences to allow for the simultaneous determination of both range and doppler velocity. Autocorrelation functions are calculated for each beam-gate cell and then fitted by standard functions to calculate the line-of sight Doppler velocity, backscattered power and width of the Doppler power spectrum. [*Greenwald et al.*, 1985; *Chisham et al.*, 2007]

SupeDARN radars also receive backscatter from the D-layer of the ionosphere or the upper mesosphere because of ionised trails of electrons due to meteor ablation in this region. *Hall et al.* [1997] first found that the backscatter in the first few range gates ('Grainy Near-Range Echoes' or GNREs) is from meteor trails at an altitude of ∼90-95 km. It is believed that approximately 1,000 tons of meteoric dust and rock enter the Earth's atmosphere each day. As a meteor enters the earth's atmosphere, the friction with the surrounding air produces enough heat to ablate the meteor and ionise the neutral air molecules, thus resulting in a long column of ionised plasma particles. Radar pulses that arrive perpendicular to the meteor trail are strongly backscattered. There are typically irregularities within the meteor

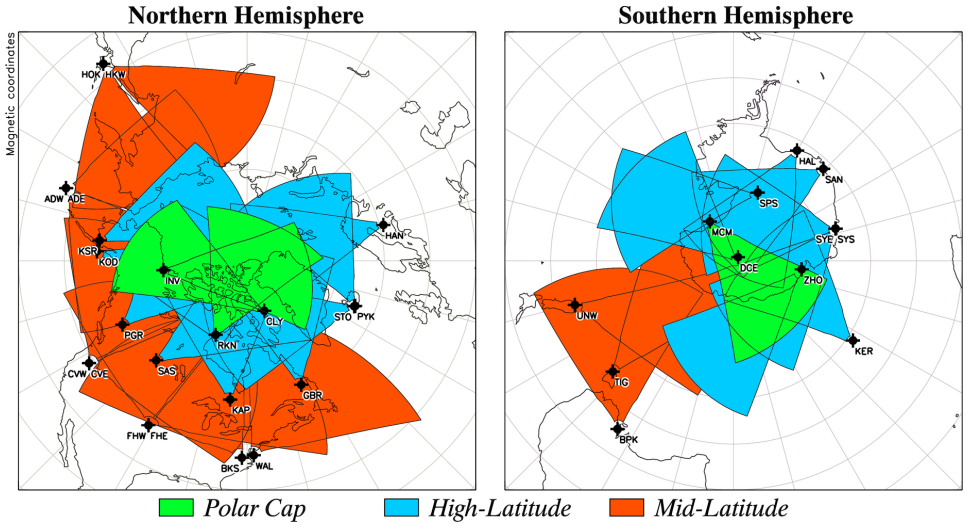

Figure 2.1: SuperDARN Radars Coverage in the Northern and the Southern Hemisphere.

trail equal to half the wavelength of HF radar signal. Figure 2.3 shows how backscatter can be obtained from a meteor trail for a bistatic radar arrangement.

The number of meteors entering the Earth's atmosphere has a prominent diurnal variation. This is because only the meteors travelling faster than Earth and in the same direction will be detected on the dusk side, whereas on the dawn side or leading edge of the Earth, meteors travelling slower than the Earth will also be detected. The motion of these ionised trails is influenced by the neutral winds in the MLT region.

2.1.1 SuperDARN MLT Wind Measurement

The meteor echoes observed by SuperDARN radars can be used to derive wind velocities in the MLT region [*Jenkins et al.*, 1998]. A sizeable component of echoes generated in the first 3 or 4 range gates (extending out to about 405 km) of a radar are presumed to be due to meteor trails that drift horizontally because of neutral winds [*Hall et al.*, 1997]. Thus, a near-range line-of-sight (LOS) velocity measurement can be used to infer a component of MLT wind velocity. We assume that the same neutral wind (constant direction and magnitude and entirely horizontal) is present over the entire area covered by the radar beams (usually

Figure 2.2: SuperDARN Radar at Blackstone.

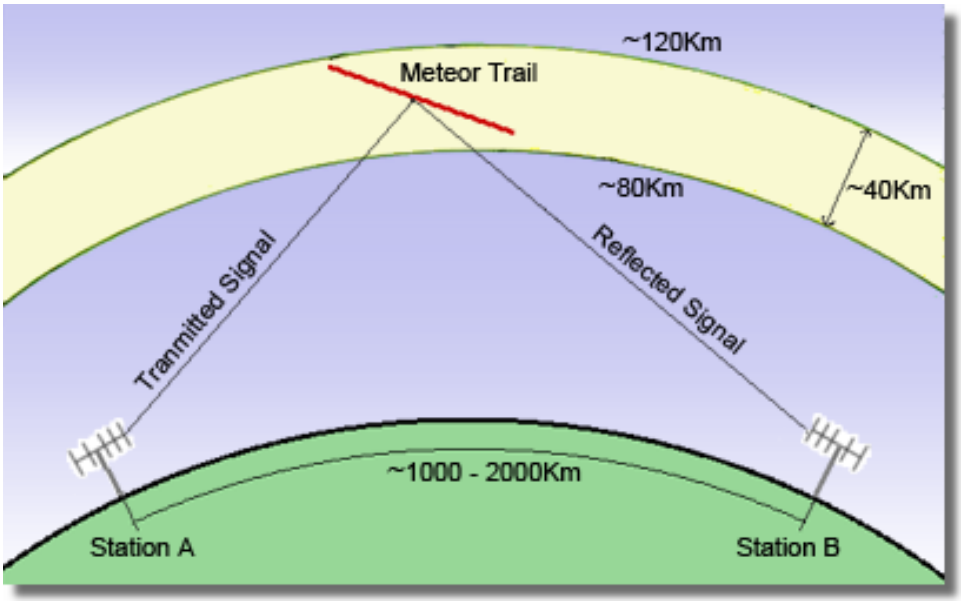

Figure 2.3: Radar Backscatter from meteor trails.

16) extending out to the outer range limit for meteor scatter. We further assume that the wind has a well-defined average velocity within one-hour UT time intervals. Then, all the meteor measurements collected during a UT hour can be used to determine a single value of neutral wind velocity for that hour and that radar. Solving for the wind velocity amounts to finding values for geographic northward (v_n) and eastward (v_e) components that best fit the set of LOS velocity measurements v_{los}. Each LOS velocity measurement is associated with a particular direction of the radar k vector in the scattering volume that can be specified by azimuth (with respect to geographic north) and elevation (with respect to the plane of the horizontal). The direction of the k vector depends only on beam and gate, but not on time. Deriving the wind-velocities requires some filtering and pre-processing steps as follows:

- Data Selection: Echoes having line of sight velocity less than 50 m/s, spectral width greater than 1 m/s but less than 50 m/s, power greater than 3 dB but less than 24 dB, and error in velocity less than 50 m/s are taken as meteor echoes and subsequently used in deriving the wind velocities. Figure 2.4 shows the field of view of the Saskatoon SuperDARN radar and the first few range gates containing meteor backscatter. The color represents the backscattered power in dB according to the scale on the right.

- Hourly Averaging: For determining hourly velocities, median line-of-sight velocities are calculated separately for all four range gates and for all beams during each hour (first four panels of Figure 2.5). We only use those range-beam cells that have echoes more than 30% of the time during that one hour.

- Elevation Scaling: The measured v_{los} implies a wind velocity component in the plane of the horizontal that is given by:

  $v_{hor} = v_{los}/cos(el)$

  Values of el at each range gate are calculated based on an assumed height of meteor backscatter of 95 km and vary from 28° at a nearest range of 185 km to 13° at a furthest range of 405 km. The back-projection factor cos (el(gate)) thus extends from 1.13 to 1.03. All velocities for each beam and gate are elevation-scaled according to the above formula to produce horizontal velocities.

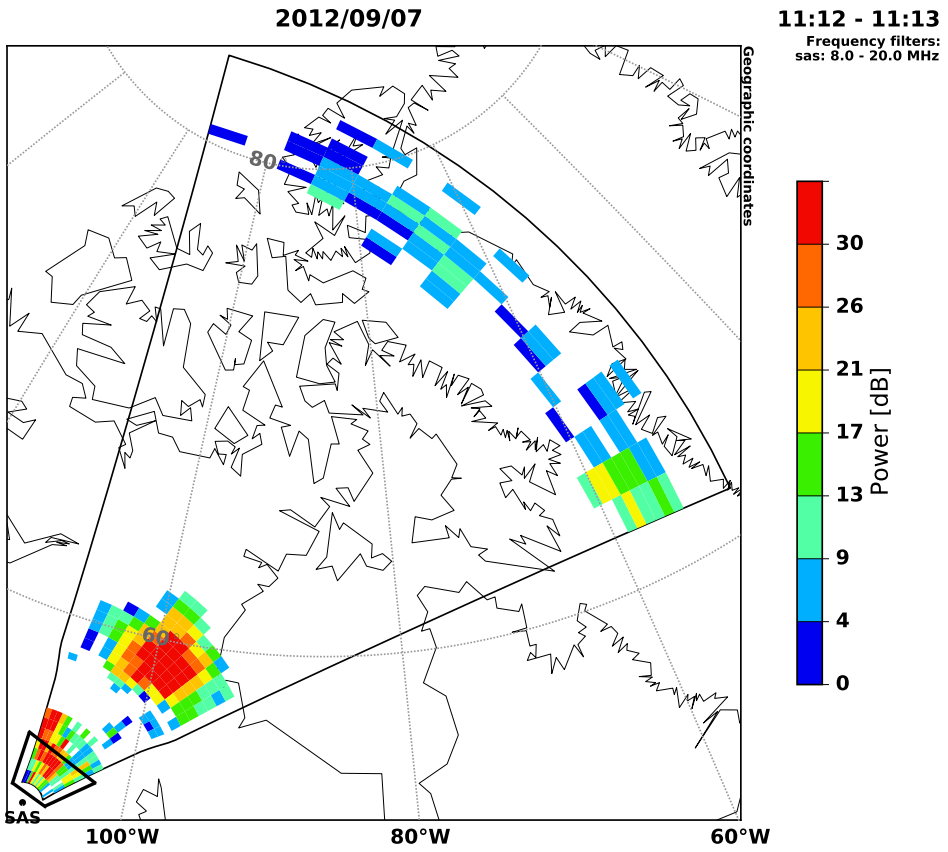

Figure 2.4: Azimuth scan of backscattered power measured by the Saskatoon radar at 11:12-11:13 UT on September 7, 2012, color coded in dB according to the scale at right. Black polygon in the near-ranges identifies meteor backscatter.

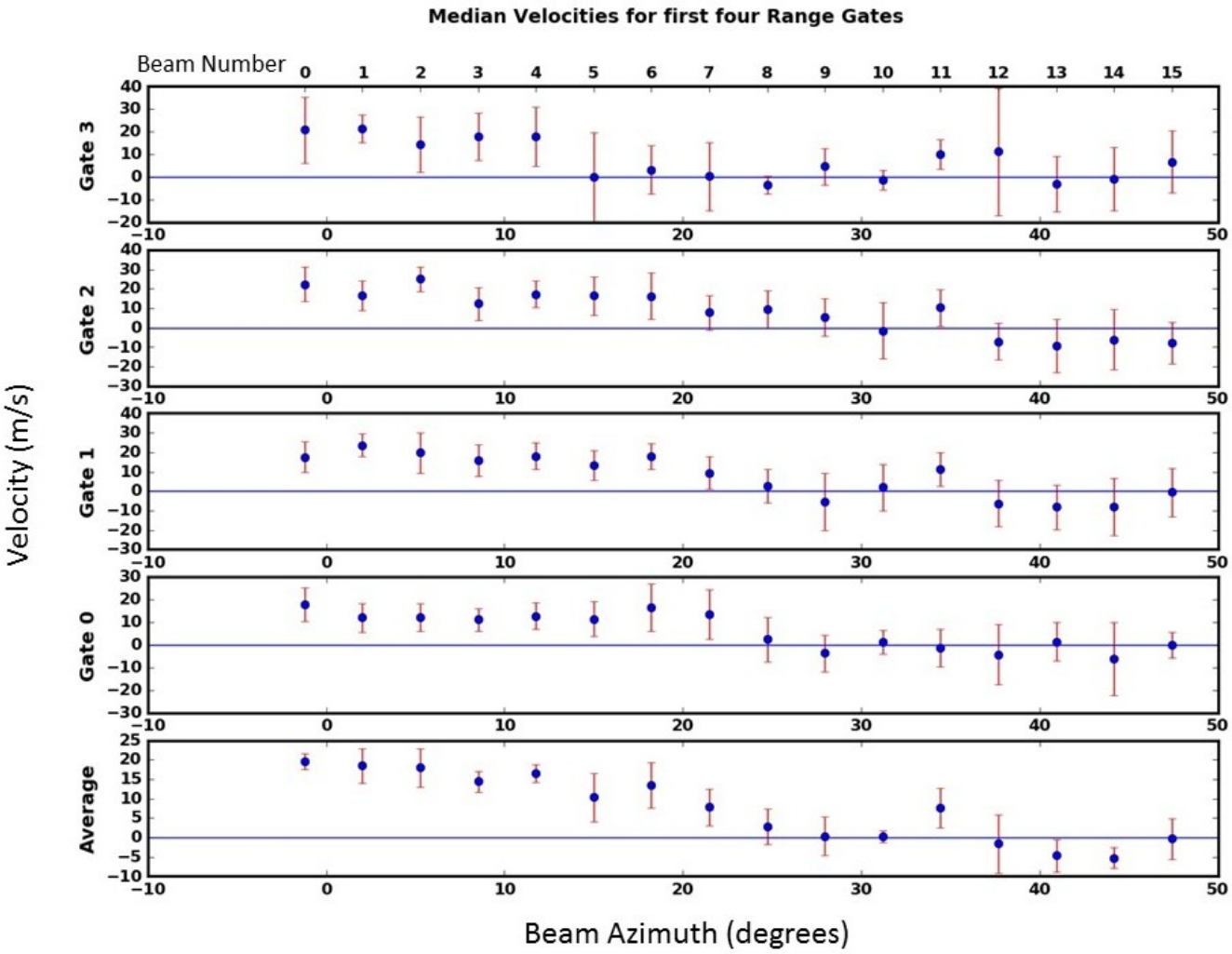

Figure 2.5: Median velocities for 1 hour for first four range gates vs beam azimuth. The vertical axis represents the velocity in m/s and horizontal axis represents the beam azimuth in degrees. From the top panel, Gate 3 median velocities, followed by Gate 2 in the second panel, Gate 1 in the third panel, and Gate 0 in the fourth panel. The bottom panel is the average of all the above four range gates, and is used for fitting with azimuth angle of each beam, to calculate the meridional (v_n) and zonal (v_e) wind velocities. This sample analysis is for the Saskatoon radar on June 25, 2002, 14:00-14:57 UT.

- Range Averaging: The horizontal velocities are then averaged over the four range gates for each beam, resulting in 16 velocity values (i.e. one for each beam) for every hour. (last panel in Figure 2.5)

- Azimuth Fitting: To proceed to a fitting for v_n and v_e, we associate each of the horizontal velocities with an azimuth by simply picking the geographic azimuth (az) for each beam (Figure 2.6).

  $v_{hor}(beam) = v_n * cos(az(beam)) + v_e * sin(az(beam))$

  We proceed to perform a least-squares fitting of the variation of v_{hor} with az to obtain v_n and v_e. The number of points available for the azimuth fitting must be greater than 5. We use a singular value decomposition routine in Python to perform the fitting. We also calculate the standard errors in the parameters calculated, v_n and v_e, as well as the r-squared goodness. Because the radars usually sweep through the meridional direction, v_n is determined more reliably than v_e.

- Outlier Analysis: We also perform an outlier analysis and remove any points that are two standard deviations away from the fitted line and continue with fitting until all the points lie within two standard deviations of the fitted line. The final outputs of the procedure are the zonal and meridional components of MLT wind velocities subject to limits on the number of points dropped (Figure 2.7). The signs of these velocities are then changed according to the look direction of the radar to match the conventional definition of zonal (positive eastward) and meridional (positive northward) wind velocities.

Numerous studies have studied the wind measurements made by SuperDARN radars to compare them with other co-located measurements and found good agreement [*Jenkins and Jarvis*, 1999; *Bristow et al.*, 1999; *Hussey et al.*, 2000]. These wind measurements have therefore been widely used to study MLT dynamics such as mean winds, tides, planetary waves and polar mesospheric summer echoes [*Hibbins et al.*, 2010; *Espy et al.*, 2005; *Malinga and Ruohoniemi*, 2007; *Kleinknecht et al.*, 2014a; *Ogawa et al.*, 2002]. In this research, we will use measurements from the mid-latitude radar at Saskatoon to study interannual and

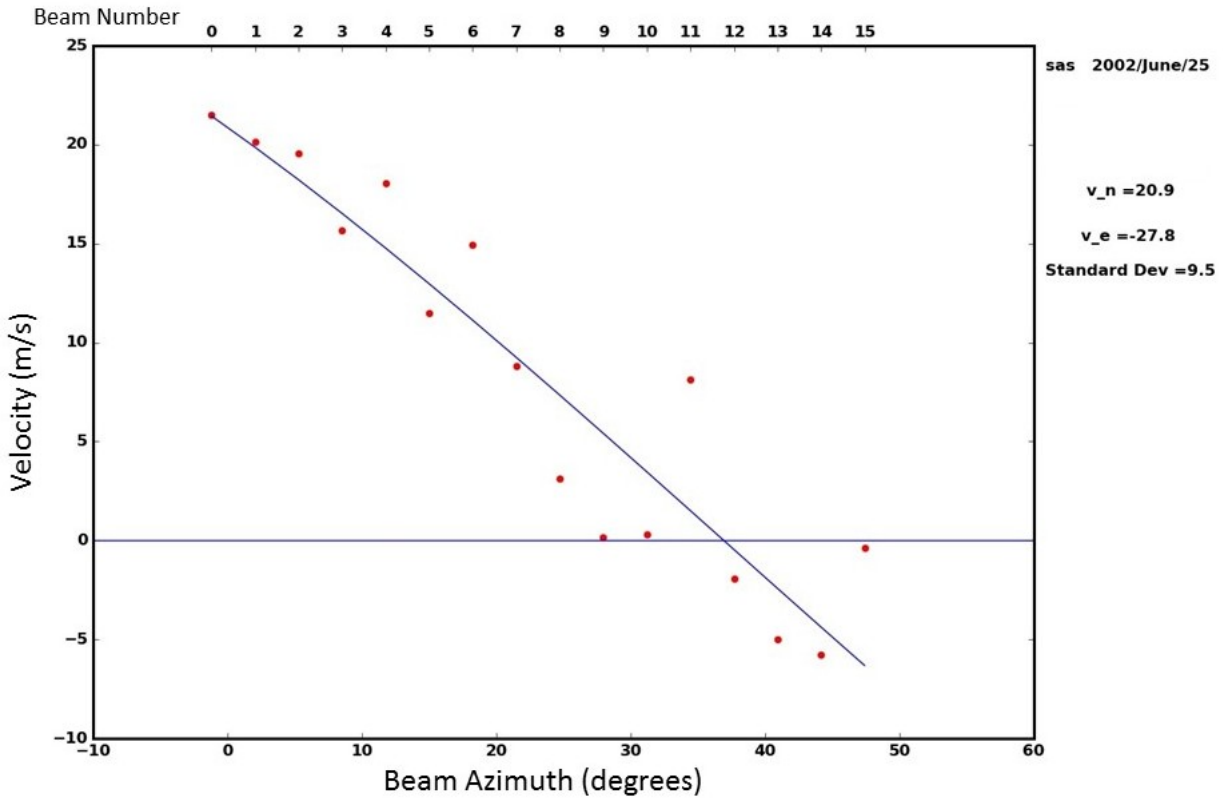

Figure 2.6: Fitting of final average elevation scaled velocities for the Saskatoon radar on June 25, 2002, from 14:00-14:57 UT. The vertical axis represents the velocity in m/s and horizontal axis represents beam azimuth in degrees. The top horizontal scale represents the beam number of the radar.

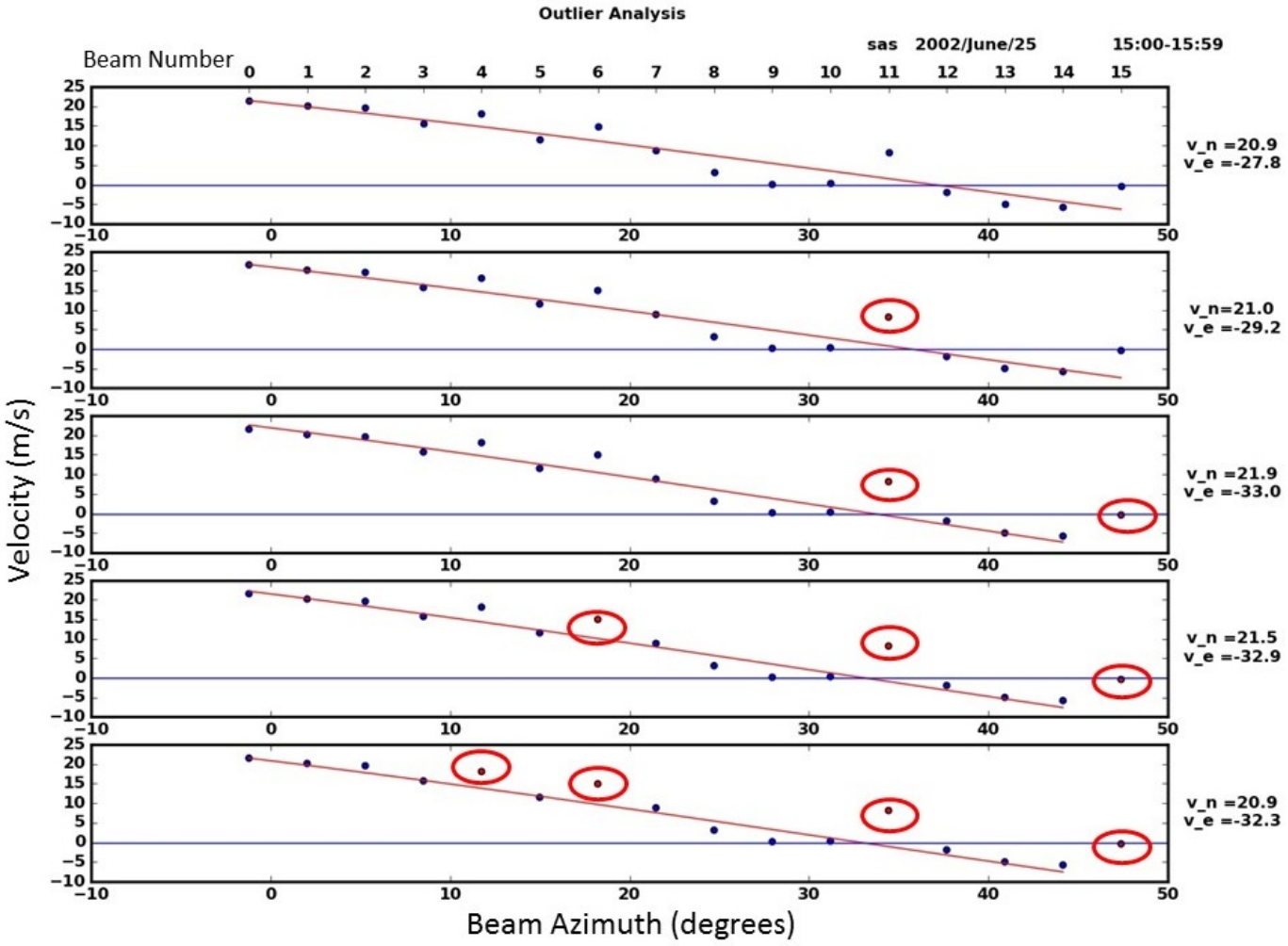

Figure 2.7: Outlier analysis to remove the points that are two standard deviations away from the fitted line. The upper panel shows the original fit to the average of four range gates. The second, third and fourth panels show the points that are not within two standard deviations being removed from the fitting analysis. The excluded points are shown in red. The vertical axis for each panel represents the velocity in m/s and horizontal axis represents beam azimuth in degrees. This sample analysis is for the Saskatoon radar on June 25, 2002, 15:00-15:59 UT.

long-term variations in the MLT neutral winds.

2.1.2 Wind Data Sample Analysis

Figure 2.8 shows the meteor echoes (top panel), and fitted zonal (middle panel) and meridional (lower panel) components of the neutral wind velocities obtained in the Saskatoon mesosphere for 24 hour period on 27 December, 2014. From the top panel, we can deduce the diurnal variation in the meteor echoes (i.e., higher in the morning hours). We can also observe a signature of semi-diurnal tides having a period of 12 hour in the wind velocity data in the lower panels.

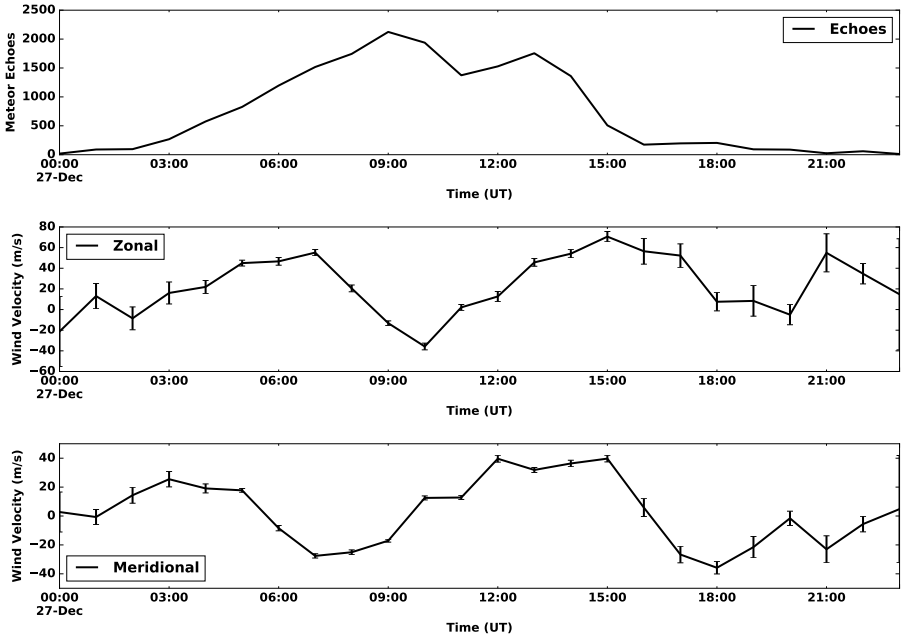

Figure 2.8: Meteor Echoes (top panel), Zonal (middle panel) and Meridional (bottom panel) wind Velocity for 27 December, 2014 at Saskatoon Radar. The vertical axis for the top panel represents the total number of meteor echoes received in the first four range gates and all the beams in an hour. The vertical axis for the middle and bottom panel represents the velocity in m/s. The horizontal axis is the Time in UT for all the panels. Local Noon is at 18:00 UTC.

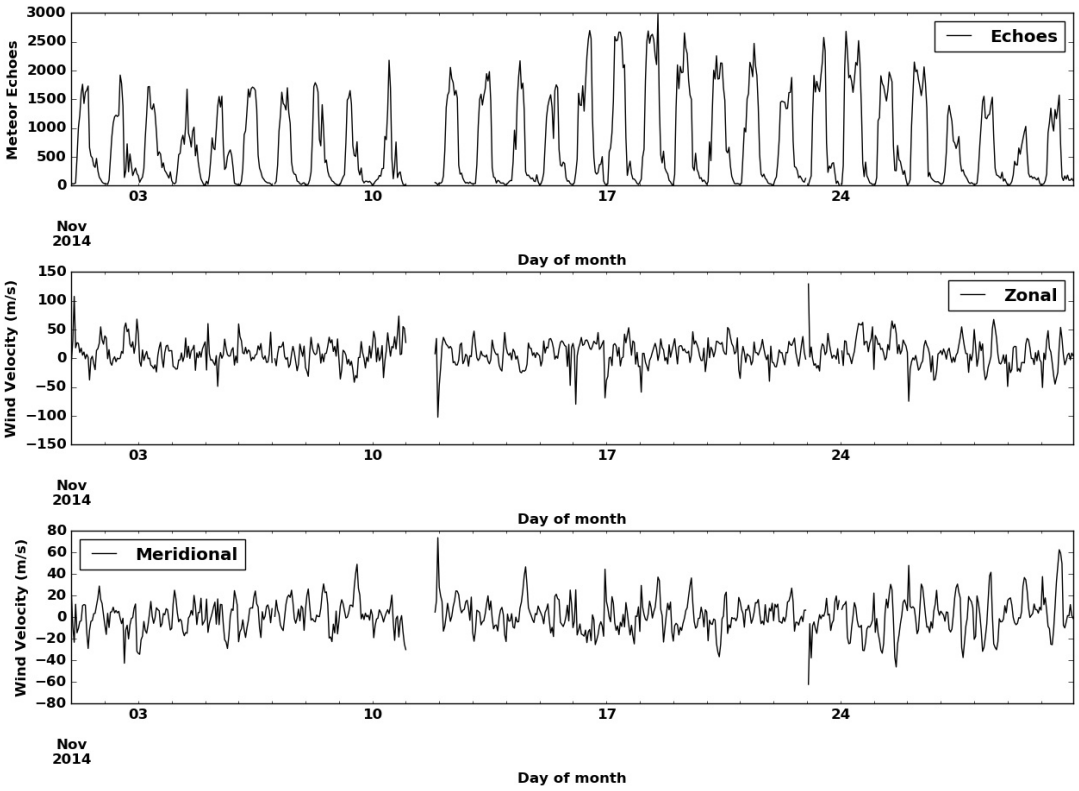

Figure 2.9: Meteor Echoes, Zonal and Meridional Wind Velocity for November, 2014 at Saskatoon Radar. The vertical axis for the top panel represents the total number of meteor echoes received in the first four range gates and all the beams in an hour. The vertical axis for the middle and bottom panel represents the velocity in m/s. The horizontal axis is the Day of month for all the panels.

Figure 2.9 is in the same format as Figure 2.8 but now shows data for the entire month of November 2014. Repeating diurnal variations can be observed in the number of meteor echoes (top panel) while Zonal and Meridional wind velocities show a much wider range of variations, ranging from hours to many days periods.

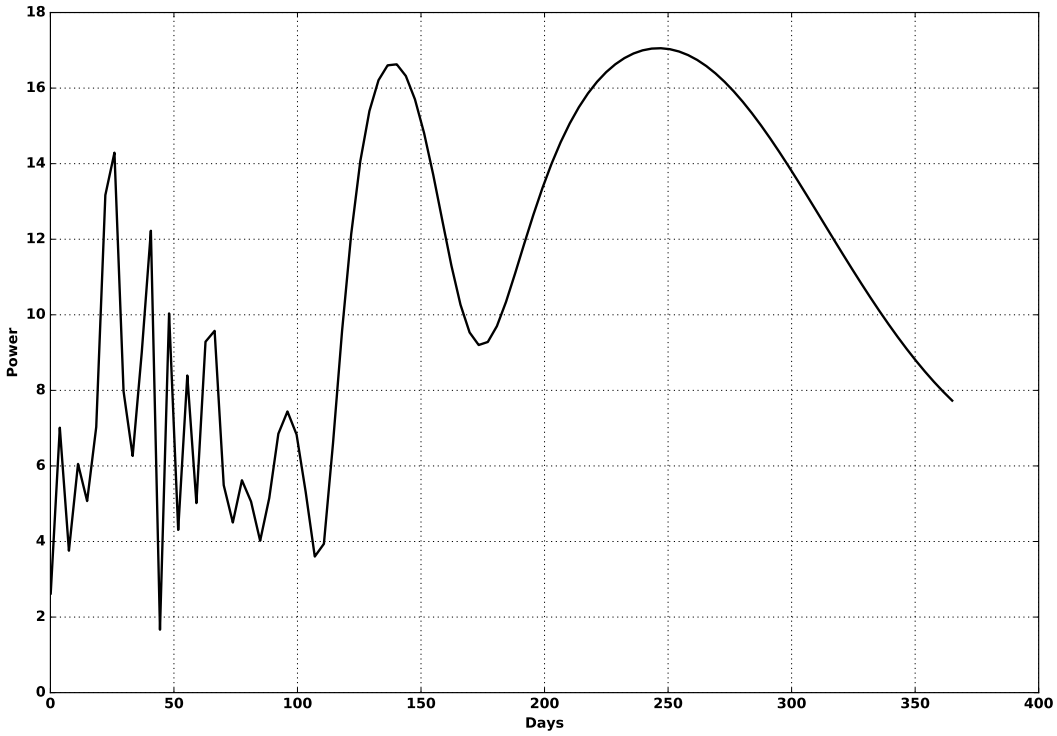

Figure 2.10: Lomb-Scargle Periodogram of 1 year of Meridional Wind Data, Saskatoon, 2014. The horizontal axis represents the period in days and the vertical axis represents the power of a particular frequency component in the wind data.

This is further investigated in Figure 2.10 which shows the Lomb-Scargle periodogram of 1 year of meridional wind data for Saskatoon (2014). The most prominent frequencies correspond to the semi-annual variation (150 days), and 27-day and 50-day planetary waves. Other peaks might be indicative of linear and non-linear interactions between various frequencies.

In this chapter we have reviewed the operation of SuperDARN radars and demonstrated basic techniques involved in determining the zonal and meridional components of neutral wind velocity at mesospheric heights. We then use this wind data to show sample plots for the Saskatoon mesosphere and observe a diurnal variation in the number of meteor echoes

and a wide range of frequencies in the zonal and meridional wind velocities. In the next chapter, we will use this data set to study the long-term variability of the winds in mid-latitude mesosphere using the SuperDARN radar at Saskatoon.

Chapter 3

HF Radar Observations of a Quasi Biennial Oscillation in Mid-Latitude Mesospheric Winds

Garima Malhotra[1], J. M. Ruohoniemi[1], J. B. H. Baker[1], R. E. Hibbins[2] and K. A. McWilliams[3]

[1] Bradley Department of Electrical and Computer Engineering, Virginia Tech, USA.

[2] Department of Physics, Norwegian University of Science and Technology, Trondheim, Norway and Birkeland Centre for Space Science, Bergen, Norway

[3] University of Saskatchewan, Canada

Corresponding author: Garima Malhotra, Electrical and Computer Engineering, Virginia Tech, VA, USA. (garima@vt.edu)

ABSTRACT

The Equatorial Quasi Biennial Oscillation (QBO) is known to be an important source of interannual variability in the mid and high-latitude stratosphere. The influence of the QBO on the stratospheric polar vortex in particular has been extensively studied. However, the impact of the QBO on the winds of the mid-latitude mesosphere is much less clear. We have applied 13 years (2002-2014) of data from the Saskatoon HF radar to show that there is a strong QBO signature in the mid-latitude mesospheric winds during the late winter months. We find that the Saskatoon mesospheric winds are related to the winds of the equatorial QBO at 45 hPa, such that the westerly mesospheric winds strengthen when QBO is easterly and vice-versa. We also consider the situation in the late-winter Saskatoon stratosphere using the ECMWF ERA-Interim reanalysis data set. We find that the Saskatoon stratospheric winds between 5 hPa and 70 hPa weaken when the equatorial QBO at 45 hPa is easterly and vice-versa. We speculate that gravity wave filtering from the QBO-modulated stratospheric winds and subsequent opposite momentum deposition in the mesosphere plays a major role in the appearance of the QBO signature in late winter Saskatoon mesospheric winds, thereby coupling the equatorial stratosphere and mid-latitude mesosphere.

3.1 Introduction

The zonal winds in the equatorial stratosphere exhibit a marked Quasi Biennial Oscillation (QBO) that is characterized by switching between easterlies and westerlies with an average period of ∼28 months [*Reed*, 1965; *Naujokat*, 1986; *Baldwin et al.*, 2001; *Kawatani and Hamilton*, 2013]. The QBO was discovered independently by *Reed et al.* [1961] and *Ebdon* [1960] and is an important mode of interannual variability in the tropics. The easterly and westerly shears originate at ∼3 hPa (∼35-40 km) and propagate downward with a speed of ∼1-2 km/month until they dissipate near ∼90 hPa (∼18 km) [*Reed et al.*, 1961; *Baldwin and Dunkerton*, 1998]. QBO is zonally symmetric and is strongest at the equator with a Gaussian-like latitudinal half-width of ∼12° [*Wallace*, 1973; *Baldwin et al.*, 2001]. Numerous modeling and simulation studies have established that its generation mechanism is an interaction between equatorial gravity waves and the background mean flow [*Lindzen and Holton*, 1968; *Holton and Lindzen*, 1972; *Plumb and Bell*, 1982; *Dunkerton*, 1997]. Even though QBO is a tropical phenomenon, it is observed to modulate the extratropical circulation in mid- as well as high-latitudes [*Sprenger and Schminder*, 1968; *Belmont and Nastrom*, 1979; *Holton and Tan*, 1980; *Dunkerton and Baldwin*, 1991; *Baldwin and Dunkerton*, 1998]. Specifically, the interannual variation of the winter polar vortex due to QBO has been the subject of studies since the 1980s [*Holton and Tan*, 1980; *Dunkerton and Baldwin*, 1991; *Baldwin and Dunkerton*, 1998].

The relationship between the polar vortex and equatorial stratospheric QBO is widely known as the Holton-Tan relationship, in which the easterly phase of QBO (∼50 hPa) results in a warmer and weaker polar vortex. *Holton and Tan* [1980] first described a mechanism to explain this synchronization between QBO and polar stratospheric winds using 16 years of geopotential height data in the Northern Hemisphere. They proposed that easterly QBO (∼50 hPa) shifts the zero-wind line into the subtropics of the winter hemisphere, narrowing the waveguide for planetary-wave propagation, resulting in poleward refraction of planetary waves and hence, a disturbed polar vortex. By contrast, westerly QBO causes the planetary waves from the extratropics to leak into the summer hemisphere, resulting in a colder, more stable vortex in the winter hemisphere. Though plausible, this mechanism has not

been adequately verified due to inconclusive observations of QBO modulation of planetary wave fluxes [*Holton and Tan*, 1980, 1982; *Dunkerton and Baldwin*, 1991] and several other mechanisms have been suggested to explain the HT relationship [*Gray et al.*, 2001b,a; *Pascoe et al.*, 2006; *Naoe and Shibata*, 2010; *Garfinkel et al.*, 2012]. Some studies have also observed modulation of the HT relationship by the 11 year solar cycle [*Labitzke and Loon*, 1988; *Gray et al.*, 2004; *Lu et al.*, 2008, 2009].

The existence of the QBO is not just limited to the stratosphere but extends into the mesosphere as well [*Burrage et al.*, 1996]. Mesospheric QBO (MQBO) maximizes at the equator but extends to $\pm 30^{\circ}$ latitudes [*Burrage et al.*, 1996]. Equatorial MQBO maximizes during the spring equinox and is opposite in phase with the stratospheric QBO [*Venkateswara Rao et al.*, 2012]. It is most probably generated by momentum deposition of gravity waves selectively filtered by the stratospheric winds [*Mayr et al.*, 1997; *de Wit et al.*, 2013]. At high-latitudes, a mesospheric QBO signal has been previously observed in planetary wave activity [*Espy et al.*, 1997; *Hibbins et al.*, 2009], semidiurnal tides [*Jarvis*, 1996; *Hibbins et al.*, 2007, 2010], diurnal tides [*Xu et al.*, 2009], temperatures [*Espy et al.*, 2011; *Mayr et al.*, 2009] and winds [*Ford et al.*, 2009; *Hibbins et al.*, 2009]. However, at mid-latitudes, the mesospheric QBO signal is comparatively less understood. Its amplitude and period have been observed to vary between 1-7 m/s and 22-36 months, respectively [*Sprenger and Schminder*, 1968; *Groves*, 1973; *Sprenger et al.*, 1975; *Neumann*, 1990; *Namboothiri et al.*, 1994; *Kane et al.*, 1999]. *Belmont and Nastrom* [1979] and *Manson et al.* [1981] reported a weak QBO in the Saskatoon mesosphere with a 180° phase shift between 75 and 105 km. *Namboothiri et al.* [1993] found a biennial periodicity in the winds at Saskatoon but could not link it to the equatorial QBO due to an inconsistent phase relationship. *Kürschner and Jacobi* [2003] found a QBO effect in mesospheric winds at Collm ($\sim 50^{\circ}$N) in phase with stratospheric winds at 30 hPa. However, several studies have searched for, but been unable to find, a robust QBO signal [*Middleton et al.*, 2002; *Baumgaertner et al.*, 2005]. Thus, the relationship of mid-latitude mesospheric QBO to equatorial QBO and its generation mechanism remains unclear.

This study aims to investigate the extent to which a QBO signature appears in the mid-latitude mesospheric winds measured by the SuperDARN HF radar at Saskatoon (52.16°N,

-106.53°E). We demonstrate the existence of such a signature and investigate its correlation with the equatorial QBO and its seasonal dependence and discuss its possible source. This paper is organised as follows: Section 2 describes the data sets employed and how they were pre-processed, Section 3 describes the results obtained by comparing the Saskatoon winds with equatorial measurements and Section 4 discusses and interprets these results followed by Section 5 which gives the Conclusions.

3.2 Data sets and Pre-processing

3.2.1 Saskatoon SuperDARN radar: Mid-Latitude Mesospheric Winds

The primary data set relates to the prevailing mesospheric winds measured by the HF radar located at Saskatoon (52.16°N, -106.53°E). This radar belongs to the Super Dual Auroral Radar Network (SuperDARN) which is a network of 30+ HF radars distributed across various sites in the mid to high latitude regions of the Northern and Southern hemispheres. The primary purpose of SuperDARN is to study plasma convection in the ionosphere by receiving backscatter from magnetic field aligned plasma irregularities [*Greenwald et al.*, 1985]. This study makes use of the 'Grainy Near-Range Echoes' (GNREs) observed in the first few range gates which are backscattered from meteor ionization trails at ∼95 km altitude [*Hall et al.*, 1997]. The longest and most reliable time series of such measurements is from the radar at Saskatoon which has been operating almost continuously since 1994. Figure 3.1 shows backscatter on beam 13 of the Saskatoon radar on September 7, 2012. The parameters from top to bottom are backscattered power, Doppler velocity and width of the Doppler spectrum with the vertical axis representing the slant range from the radar and the horizontal axis representing universal time. Black ellipses between 8:00 UT to 13:00 UT highlight the ranges of meteor backscatter. Meteor backscatter spans the near-range gates and has a peak during local midnight and early morning hours. Weaker meteor backscatter can be observed outside this time interval. Ranges further than these are dominated by ionospheric

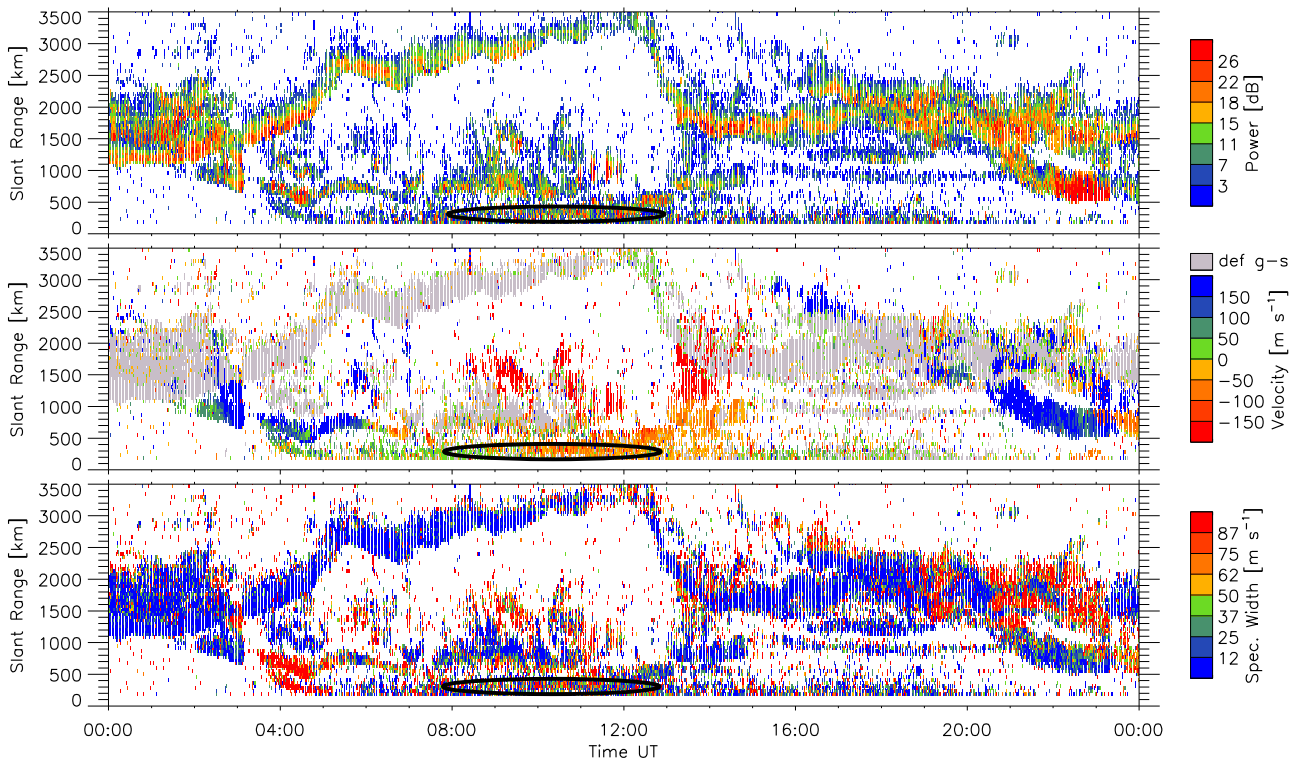

Figure 3.1: Backscatter on beam-13 measured by the Saskatoon radar on September 7, 2012. Parameters from top to bottom are backscattered power, Doppler velocity and width of the Doppler spectrum. The vertical axis represents the slant range from the radar and the horizontal axis represents Universal Time. Black ellipses highlight near-range meteor backscatter.

and ground backscattering. Figure 3.2 shows an azimuth scan covering all 16 beams which completed at 11:13 UT with colors representing the backscattered power. The black polygon is the region in which backscatter from meteors can reliably be used to derive wind velocities in the mesosphere. The backscatter at ranges just beyond those of the highlighted region is from E-region irregularities [*Chisham et al.*, 2007]. The backscatter from the furthest ranges in Figure 3.2 is due to ground scatter associated with reflection from the F region.

The meteor echoes observed by the SuperDARN radars can be used to derive wind velocities at mesospheric heights [*Jenkins et al.*, 1998]. Extracting hourly mean zonal and meridional components of the mesospheric winds from the Saskatoon radar meteor echoes requires some pre-processing steps to isolate them from other forms of backscatter and to remove noise.

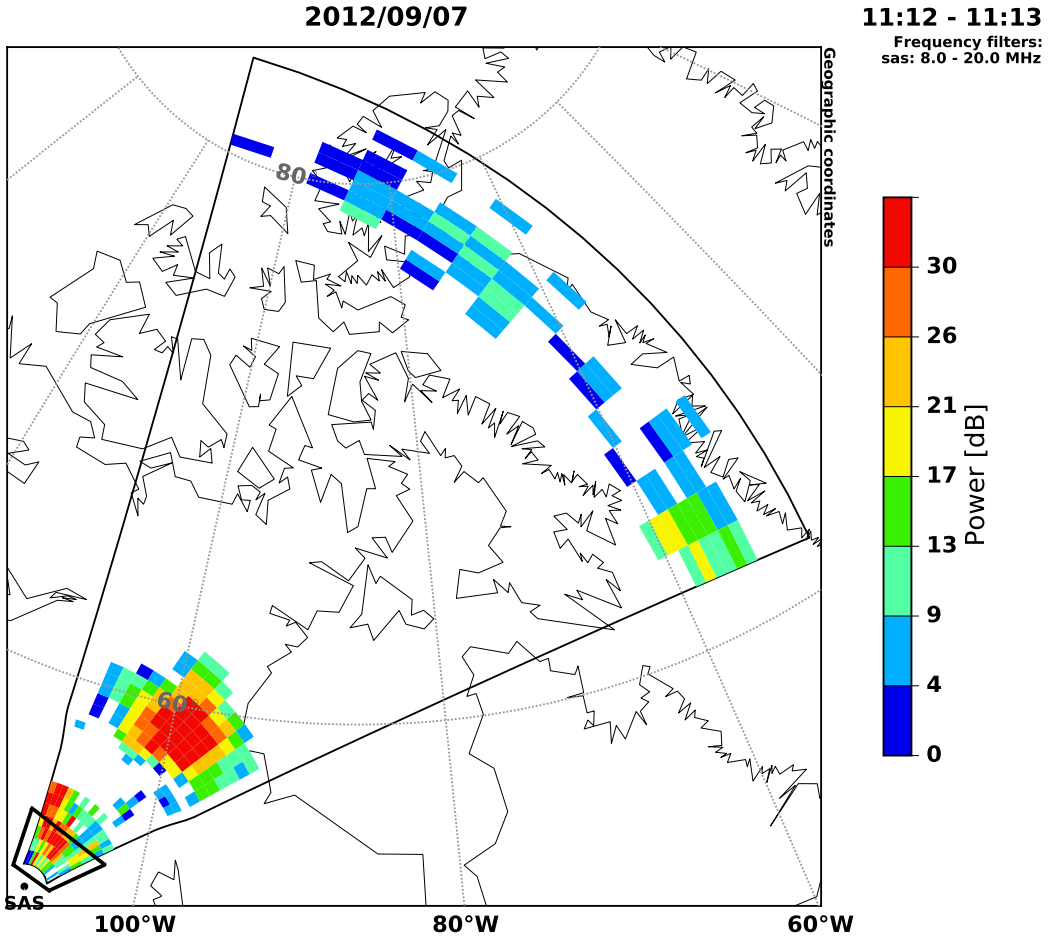

Figure 3.2: Azimuth scan of backscattered power measured by the Saskatoon radar at 11:12-11:13 UT on September 7, 2012, color coded in dB according to the scale at right. Black polygon in the near-ranges identifies meteor backscatter.

Specifically, we have excluded echoes having line of sight velocity greater than 100 m/s, error in velocity greater than 50 m/s [*Hibbins et al.*, 2009], spectral width less than 1m/s or greater than 50 m/s and signal to noise ratio less than 3 dB or greater than 24 dB [*Matthews et al.*, 2006]. The remaining echoes are assumed to represent backscatter from meteor ionization trails and are used to calculate hourly median velocities over the first four range gates. The median line-of-sight velocity for each beam-gate cell is then scaled by the elevation angle to obtain horizontal velocities. The analysis assumes that the same neutral wind vector is present over the entire area covered by the radar beams and the wind has a well defined average velocity within the one-hour UT intervals. Hourly median horizontal velocities in the first four range gates are averaged for each beam resulting in 16 velocity values for every hour. These azimuthally distributed velocities are then fit using least squares singular value decomposition over all radar beam azimuth angles [*Press et al.*, 1992]. The fitting is performed for those hours having data in at least five radar beams. Previous studies have used a similar technique to derive mesospheric winds from the SuperDARN radars [*Jenkins et al.*, 1998; *Jenkins and Jarvis*, 1999; *Bristow et al.*, 1999; *Hussey et al.*, 2000; *Malinga and Ruohoniemi*, 2007; *Hibbins et al.*, 2007].

The last step is to produce a daily zonal wind using a technique similar to that used by *Hibbins and Jarvis* [2008]. Specifically, hourly zonal winds are split into 4-day segments and a running non-linear least squares fit anaysis is done to remove the high frequency components of terdiurnal (8 hour), semidiurnal (12 hour), diurnal (24 hour) tides and the quasi two day (48 hour) planetary wave. To ensure a good fit, only those data segments having more than half of the hourly winds are used. This running fit analysis is successively stepped by one day to create a time series of the daily zonal winds. Monthly mean winds are then calculated by averaging the daily zonal winds. The measurements span the 2002-2014 interval.

Previous studies have compared the winds derived from SuperDARN radars with measurements of other co-located instruments and found good agreement at mesospheric altitudes of ∼90-95 km [*Bristow et al.*, 1999; *Hussey et al.*, 2000]. Over the past decade, the SuperDARN radars have been used to study several prominent mesospheric phenomena such

as the Quasi Two Day planetary wave [*Malinga and Ruohoniemi*, 2007], polar mesospheric summer echoes [*Ogawa et al.*, 2004], long-period planetary waves [*Espy et al.*, 2005; *Hibbins et al.*, 2009; *Kleinknecht et al.*, 2014b] and semidiurnal tides [*Hibbins et al.*, 2007; *Hibbins and Jarvis*, 2008].

3.2.2 ERA Interim-ECMWF: Mid-Latitude Stratospheric Winds

To assess the QBO signature in the mid-latitude stratosphere, winds are specified using monthly mean zonal wind data from the European Centre for Medium-Range Weather Forecasts (ECMWF) Re-Analyses (ERA) Interim data set. This global atmospheric reanalysis data set began in 1979, is constantly updated in real time, and is archived at 2.5°×2.5° grid spacing resolution. It uses the ECMWF Integrated Forecasting System (IFS), which incorporates a model with three fully coupled components for the atmosphere, land surface, and ocean waves [*Dee et al.*, 2011]. All observations used in ERA-Interim are subject to a suite of quality control and data selection steps [*Dee et al.*, 2011]. The forecast model, data assimilation method and input data sets used to produce ERA-Interim are described in detail by *Berrisford et al.* [2009] and *Dee et al.* [2011]. For the purposes of this study, we use the zonal winds for 2002-2014 obtained from pressure levels 1 to 70 hPa at 53.15°N and 254.52°E as an approximate measure of winds in the stratosphere over Saskatoon.

3.2.3 Singapore Radiosonde Station: Equatorial Stratospheric Winds

Winds in the equatorial stratosphere are specified using monthly mean zonal wind data obtained by the Singapore radiosonde station (1°N, 104°E). These measurements are commonly used as a proxy for the equatorial Quasi Biennial Oscillation (QBO). The data were downloaded from http://www.geo.fu-berlin.de/met/ag/strat/produkte/qbo/singapore.dat provided by Free University of Berlin. This data set has been produced since 1987 from the Singapore radiosonde measurements by using the daily vertical wind profiles. This data set is representative of the entire equatorial belt since longitudinal differences in the phase of QBO are known to be small [*Belmont and Dartt*, 1968]. For the purposes of this study, we use the

zonal winds for 2002-2014 obtained from pressure levels 10 hPa to 100 hPa.

3.3 Results

In this section, we present evidence of a QBO signature in the mid-latitude mesospheric winds measured by the Saskatoon HF radar and show that it has a significant correlation with the equatorial QBO measured in the Singapore radiosonde data, and investigate the relationship with the mid-latitude stratospheric winds derived from the ECMWF data set.

3.3.1 Zonal Wind Observations

Saskatoon Mesospheric Winds: Monthly mean zonal winds measured by the mid-latitude Saskatoon radar for 2002-2014 are presented in Figure 3.3a. A persistent seasonal cycle is apparent along with year-to-year variations. To isolate this interannual variability, the winds are first de-seasonalized in Figure 3.3b by subtracting the average climatology from the time-series in Figure 3.3a, and then a Lomb-Scargle analysis is performed to examine the frequency components in the residual winds. Figure 3.3c shows the Lomb Scargle periodogram obtained. Several peaks are visible. Of particular note for this study is the prominent peak at 27.6 months which can be associated with the Quasi Biennial Oscillation (QBO) and the peaks around 8 and 22 months which could be attributed to a non-linear interaction between the seasonal (12 month) cycle and the QBO, suggesting that the QBO signal in these data is carried preferentially in one season.

Singapore Equatorial QBO: Quasi-biennial oscillation is seen at the equator as downward propagating bands of alternating westerly and easterly winds. These features are illustrated in Figure 3.4 which shows height-resolved stratospheric monthly mean zonal winds at the Singapore equatorial radiosonde station for 2002-2014. The contour interval is 10m/s with red (blue) representing westerly (easterly) winds. A cycle of 28 months can be clearly seen along with pronounced asymmetry between the two phases such that easterly phases tend to have higher intensity (darker blues than reds) and longer duration than westerly

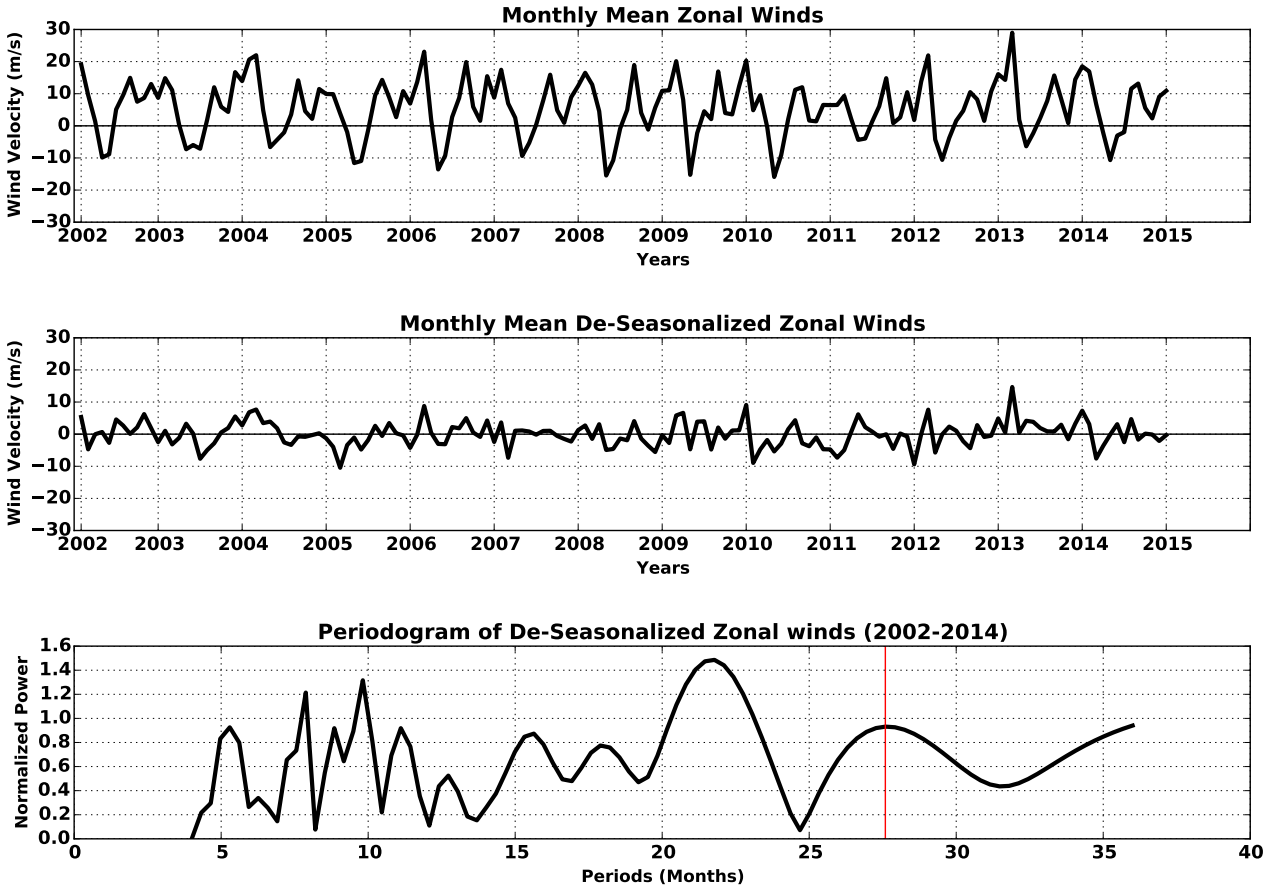

Figure 3.3: (a) Time series of monthly mean mesospheric zonal winds recorded by the Saskatoon radar for 2002-2014. Negative values indicate easterly (westward propagating) winds and positive values indicate westerly (eastward propagating) winds.(b) Time series of de-seasonalized monthly mean mesospheric zonal winds obtained by subtracting the mean climatology at Saskatoon radar from the winds in Figure 3a. (c) Periodogram for the de-seasonalized mesospheric zonal winds at Saskatoon for 2002-2014 (Figure 3b), with a red line identifying a peak at a frequency of 27.6 months.

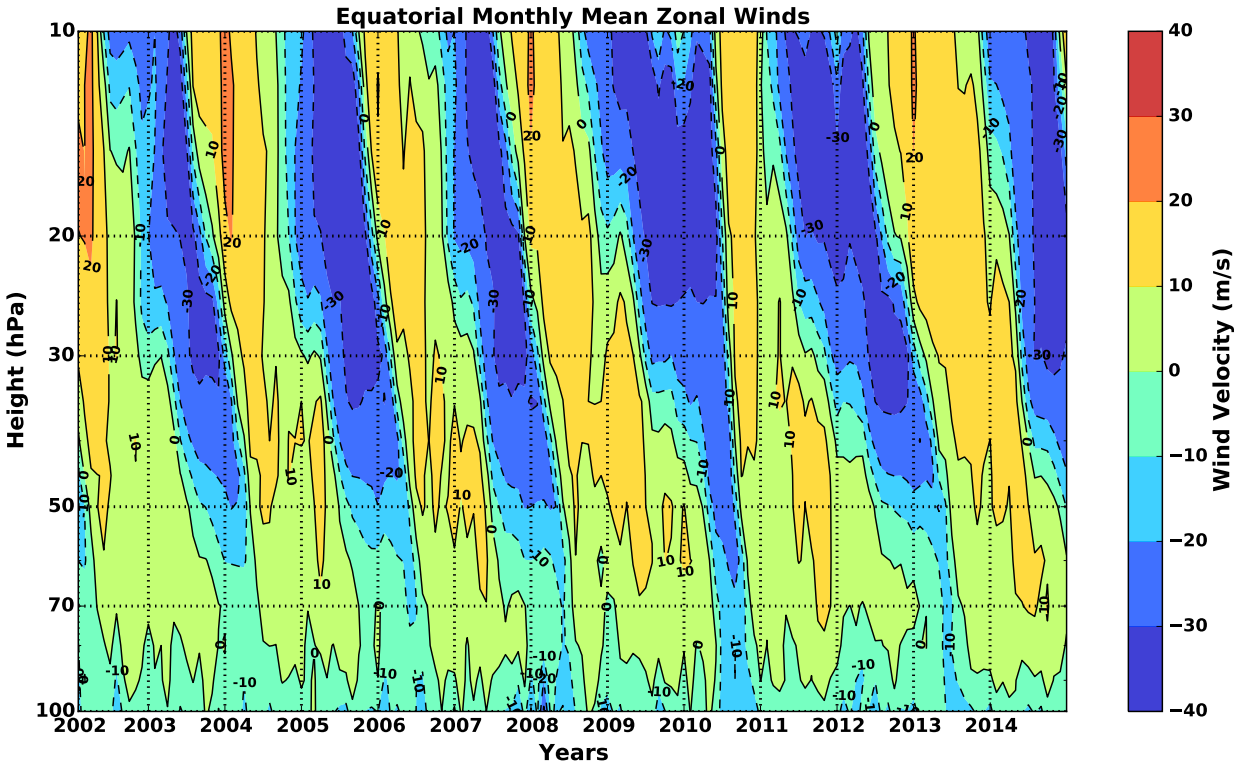

Figure 3.4: Height resolved stratospheric zonal winds at the Singapore equatorial radiosonde station for 2002-2014. The contour interval is 10 m/s with colors representing wind velocities in m/s. Red represents westerly winds, whereas blue represents easterly winds.

phases above 50 hPa. This is especially evident from 2009 onwards. At 50 hPa, most of the phase transitions occur in spring-summer months suggesting QBO is synchronized with the annual cycle at this altitude. By contrast, at about 100 hPa (∼15-20 km), QBO is much less apparent and there is instead a steady layer of easterly winds.

Comparison of this figure to Figures 3.3a and 3.3b shows that the late winter (Jan-Feb) peaks in westerly mesospheric winds (e.g., during 2004, 2006 and 2013) typically occur during easterly phases of the ∼45-50 hPa QBO. This is evidence that the mesospheric zonal wind anomalies at mid-latitudes are related to the phase of the equatorial stratospheric QBO.

QBO-ordered Climatology of Mid-Latitude Mesospheric winds: To further study

the possibility of QBO influences in the mid-latitude Saskatoon mesospheric winds, we divide the monthly mean wind data shown in Figure 3a according to QBO phase to produce a climatology of the mid-latitude zonal winds for when the QBO phase is positive at 50 hPa (shown in red in Figure 3.4) and when the QBO phase is negative at 50 hPa (shown in blue in Figure 3.4). Figure 3.5 shows the result. The blue curve is the climatology for years when QBO was easterly while the red curve is the climatology for the years when QBO was westerly. The average climatology obtained by averaging all zonal winds, is identified by the green curve. It is evident from the green curve that the mid-latitude mesospheric winds at Saskatoon are dominated by easterlies (negative values) from March to June and westerlies (positive values) during the rest of the year. During late fall and winter (Nov-Feb), the prevailing winds at Saskatoon are generally westerlies that dramatically reverse to easterlies over a one month period between February and April. The peak easterly wind velocities occur during April. These winds then reverse back to westerlies in June reaching high magnitudes of around $\sim$15 m/s in August. The winds decrease to low magnitudes of ~ 5 m/s in September and of $\sim 2-3$ m/s in October, however, they do not reverse direction. These westerly winds start increasing in magnitude from October and persist for the entire winter. This climatology agrees well with that described by *Manson and Meek* [1986] and *Portnyagin and Solovjova* [2000] at $\sim$95 km at mid-latitudes.

It can also be observed that the difference between the winds of the two QBO climatologies ranges between 0 m/s and 8 m/s. During late fall and winter (Nov-Feb) generally, when the prevailing winds are westerlies, the easterly phase (blue) of QBO increases the magnitude of the Saskatoon mesospheric winds relative to the westerly phase (red). The effect of QBO after the spring reversal, during April and May, is such that the easterly (westerly) phase of QBO increases (decreases) the magnitude of the easterly wind velocity, thus making it more (less) easterly. During August, the westerly prevailing winds decrease (increase) in magnitude when QBO is easterly (westerly), thus becoming less (more) westerly. This late summer effect of the QBO on mesospheric winds is thus opposite to that observed during winter. In September, the effect of QBO flips again and is similar to that observed in the winter. It can be noted that the QBO differences are largest during late winter (January-February).

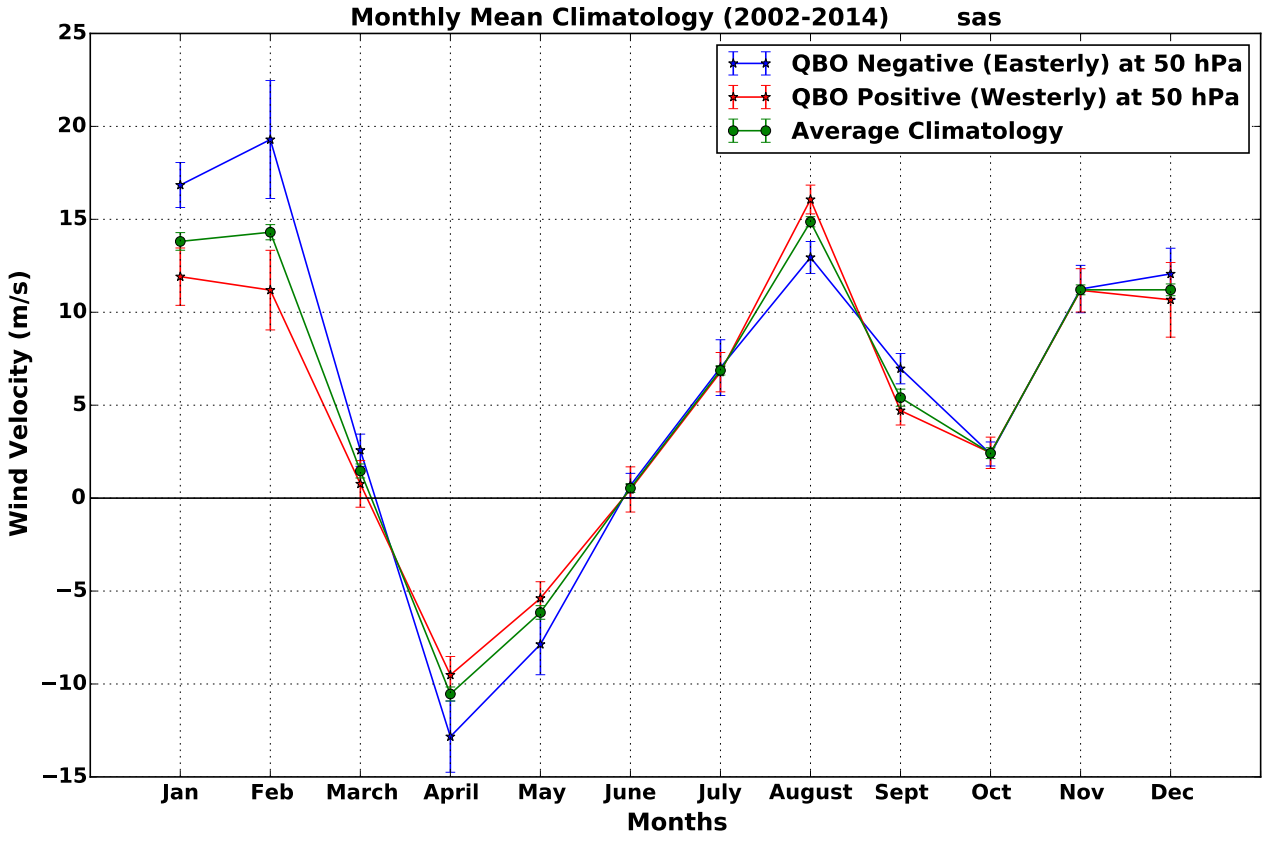

Figure 3.5: Climatology of prevailing zonal winds at Saskatoon organized by phases of QBO at 50 hPa. Green represents the climatology obtained by averaging the zonal winds in Figure 3a. Blue (red) represents the climatology for the years when QBO is easterly (westerly). Positive velocities indicate westerly winds and negative velocities indicate easterly winds.

3.3.2 Correlative Analysis: All Months

Saskatoon Mesospheric Winds vs. Singapore Stratospheric QBO: To further examine the characteristics of the QBO signal in the Saskatoon monthly mean mesospheric zonal winds (∼95 km), a height resolved correlation analysis is performed against the Singapore stratospheric QBO spanning all pressure levels (10 hPa-70 hPa), for each month. The results are shown as a correlation contour plot in Figure 3.6 with an interval of 0.1 and colors representing the correlation magnitudes. Plus symbols identify correlations having significance>90%. Each data point on this contour plot represents the correlation between two data series of 13 points (for 13 years). A feature of particular interest is the relatively high negative correlation which occurs during late winter (Jan-Feb) corresponding to the lower stratospheric QBO (40-70 hPa), whereas a positive correlation is observed at the higher altitudes (10-20 hPa). Thus, there is a sharp altitude gradient in the correlation during these months at ∼25-30 hPa. This indicates that the QBO during these months reverses its phase at these altitudes. In March, the positive correlation with the upper stratospheric QBO continues. From April to May, the region of positive correlation with QBO moves to lower altitudes of 40-70 hPa. This is followed by negligible to slightly negative correlation in June-July and hence no discernible QBO influence on the Saskatoon mesospheric winds in early summer. In August, the correlation of the winds with lower stratospheric QBO (30-50 hPa) flips again and becomes positive, with significance greater than 90%. This is opposite to that observed in late winter at lower altitudes. In September, the Saskatoon mesospheric winds exhibit negative correlation with Singapore lower stratospheric QBO followed by negligible correlation in early winter (Oct, Nov, Dec) at all altitudes of QBO. This figure implies that the Saskatoon mesospheric winds are significantly correlated with the equatorial QBO during Jan, Feb, March and Aug.

To further draw out the magnitude of the QBO effect, the two QBO climatologies are subtracted (Westerly QBO - Easterly QBO). Figure 3.7 shows a contour plot of the difference between the mid-latitude zonal winds of westerly and easterly QBO climatologies where QBO phase is defined by the direction of the winds measured by the Singapore radiosonde at different pressure levels identified on the left vertical axis. The contour interval is 1m/s

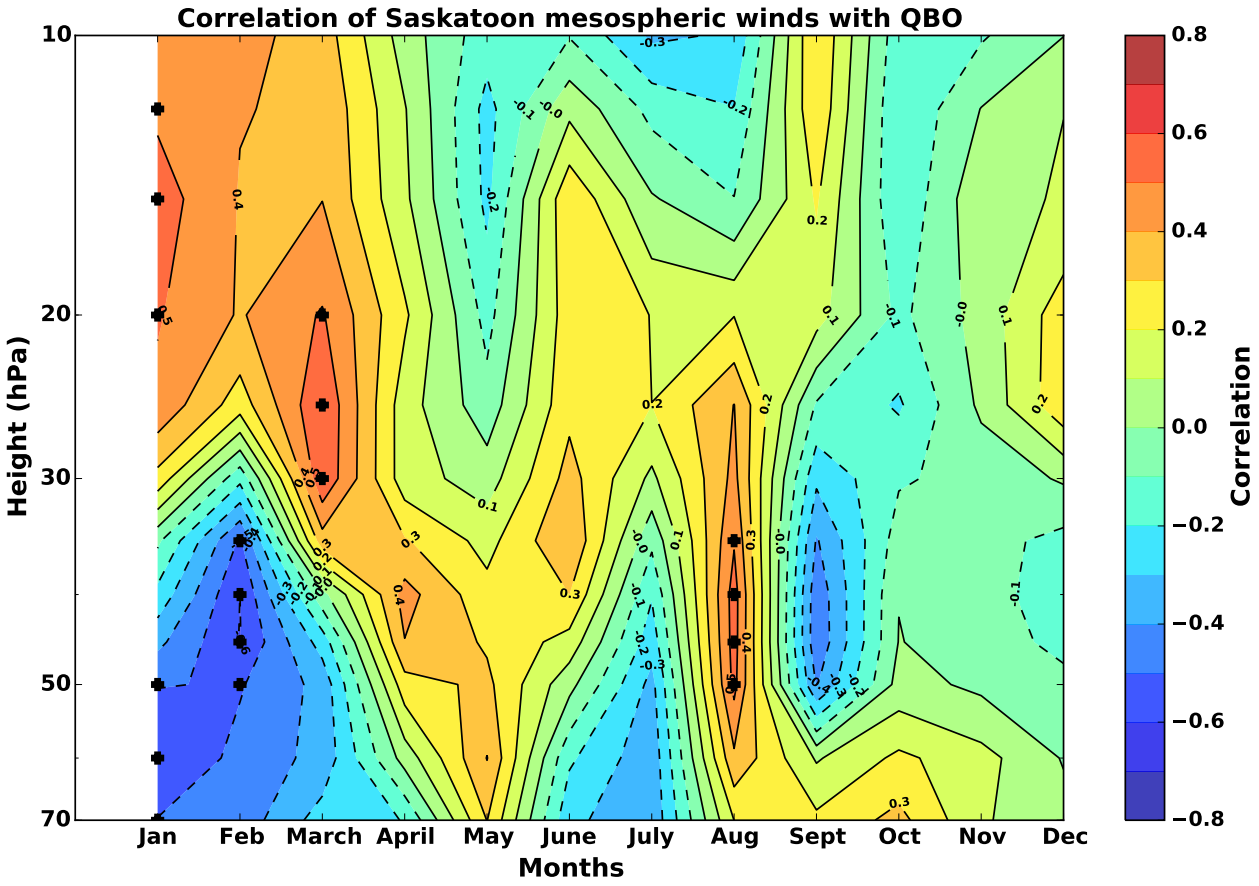

Figure 3.6: Correlation of Saskatoon mesospheric zonal winds with QBO spanning all pressure levels on the left vertical axis, for all the months. The contour interval is 0.1 with colors representing correlation magnitudes. Plus symbols identify correlations with significance greater than 90%.

and contours are colored red (blue) for positive (negative) difference magnitudes. The most striking feature is the relatively high difference in wind velocities in Jan-Feb which maximizes at 10 m/s when QBO phase is defined by ∼45 hPa winds. Only comparatively small differences (<4 m/s) are seen in other months regardless of altitude. The sharp reversal in difference magnitudes at ∼25-30 hPa in late winter indicates a phase reversal of the equatorial QBO which was also noted in Figure 3.6. Thus, the Saskatoon mesospheric winds exhibit the largest QBO signal in the radar data during late winter. We therefore investigate the winds during this time in more detail through time series analysis.

3.3.3 Correlative Analysis: Late Winter

Saskatoon Mesospheric Winds vs. Singapore Stratospheric QBO:

Figure 3.8a shows the time series of averaged late winter QBO zonal winds measured by the equatorial Singapore radiosonde at 45 hPa and Figure 3.8b shows mesospheric zonal winds measured by the mid-latitude Saskatoon radar from 2002 to 2014 through the late winter period. The positive velocities indicate westerly winds and negative velocities indicate easterly winds. The designation of all positive values in Figure 3.8b indicates that the mesospheric winds are consistently westerly during Jan-Feb, as observed before in Figure 3.5, whereas QBO in Figure 3.8a alternates between its westerly and easterly phases. The main feature of interest in Figure 3.8b is the approximately two-year periodicity in the Saskatoon mesospheric winds. The correlation between the two time series is -0.63 with a significance of ∼98%. This corresponds to the blue colored area on the bottom left (during Jan-Feb) of Figure 3.6 and 3.7. The dominant feature in this figure is that the mesospheric winds tend to strengthen (weaken) and hence become more (less) westerly when QBO at 45 hPa is easterly (westerly). However, there are some years when the variations are less distinct and this general trend is not so apparent, for example, 2009-2012 corresponds to a change in QBO structure in Figure 3.8a. This feature can also be identified in Figure 3.4. Both data sets exhibit more irregular behavior through these years.

Saskatoon Stratospheric Winds vs. Singapore Stratospheric QBO:

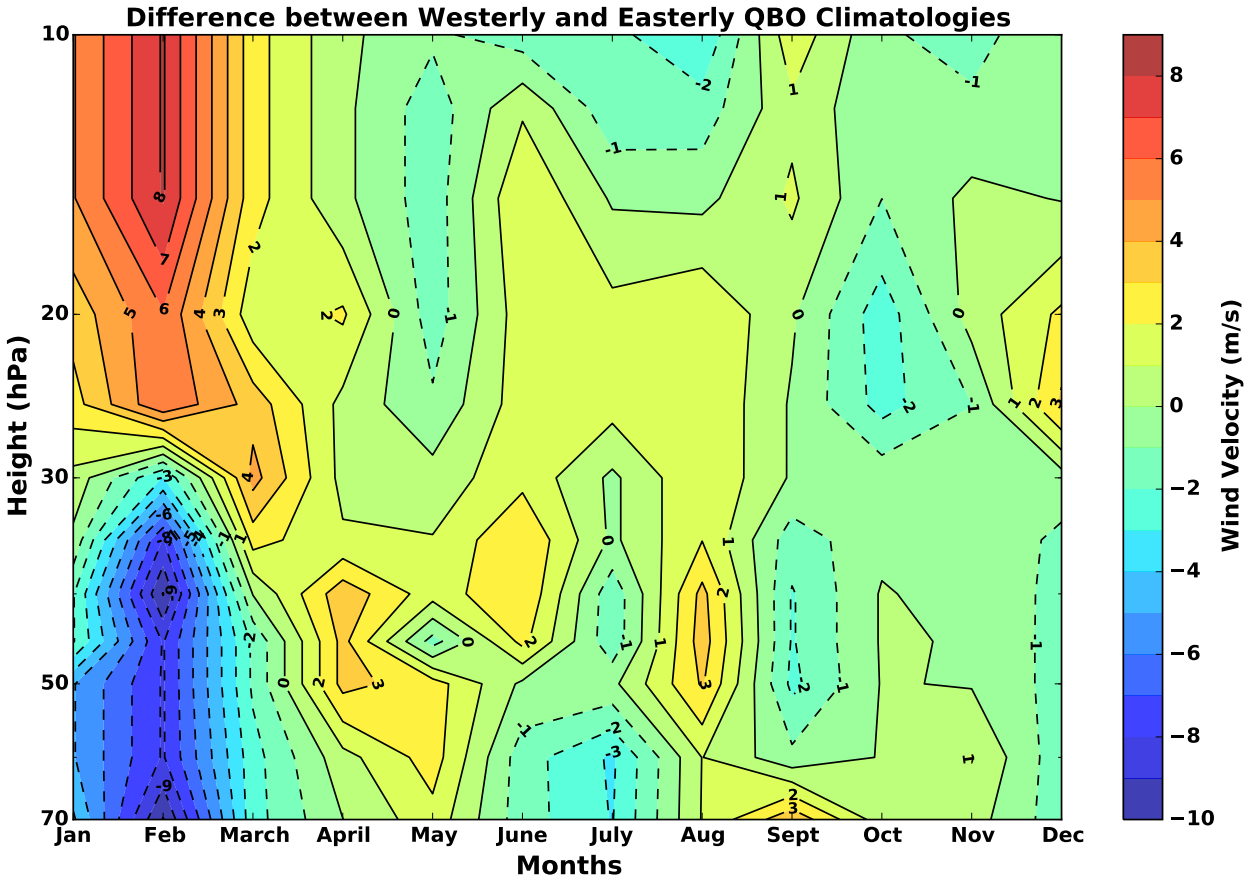

Figure 3.7: Difference between Westerly and Easterly climatologies of the zonal winds at Saskatoon organized by QBO phase. QBO phase is defined by the direction of the winds measured at Singapore for the different pressure levels identified on the left vertical axis. The contour interval is 1 m/s and contours are colored red (blue) for positive (negative) difference.

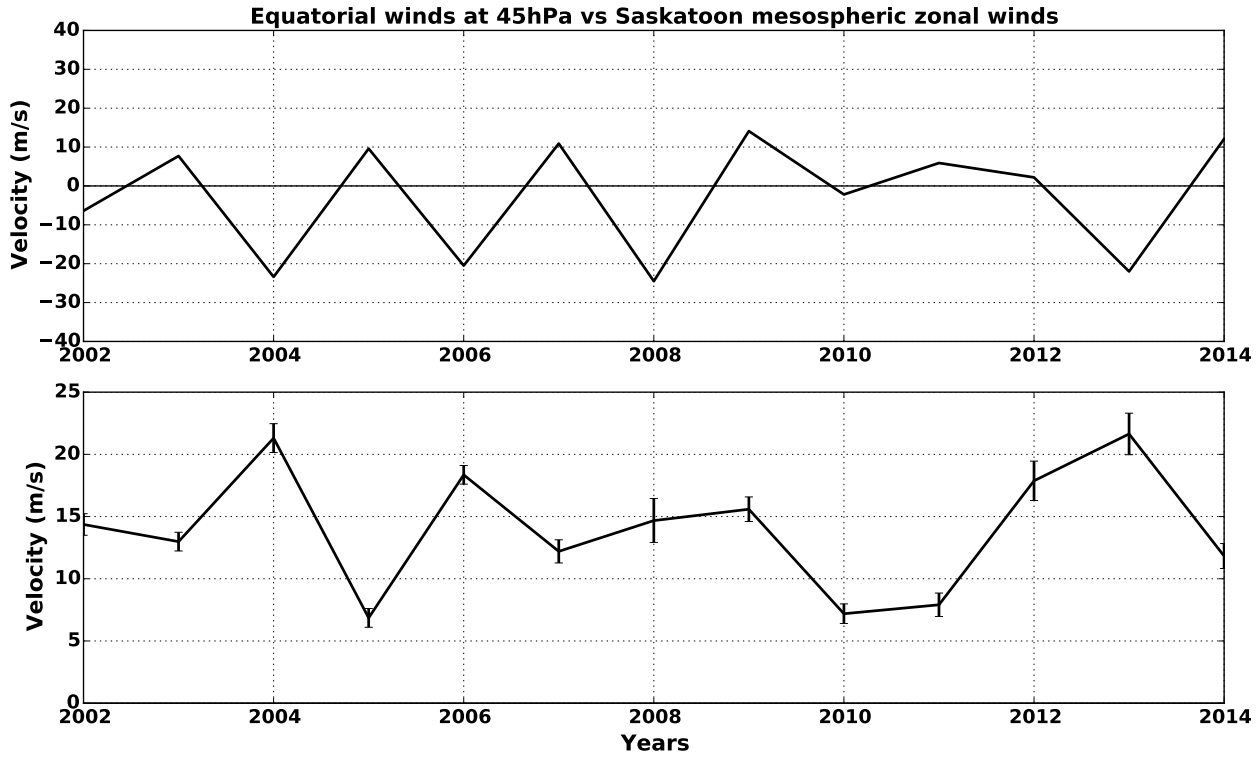

Figure 3.8: (a) Averaged late winter (Jan-Feb) zonal winds measured by the Singapore radiosonde at 45 hPa for 2002-2014. (b) Averaged late winter (Jan-Feb) mesospheric zonal winds measured by the Saskatoon HF radar for 2002-2014. For both the figures, positive velocities indicate westerly winds and negative velocities indicate easterly winds.

Unlike its influence on the mid-latitude mesosphere, the QBO is widely known to modulate the stratospheric polar vortex winds and planetary wave fluxes in the winter hemisphere [*Holton and Tan*, 1980; *Anstey and Shepherd*, 2014], although the consistency of the Holton-Tan relationship over time has been found to be variable [e.g., *Naito and Hirota*, 1997; *Lu et al.*, 2008] especially over late winter. It is also widely known that the mesospheric circulation is primarily driven by momentum flux deposition of near-vertically propagating gravity waves filtered by the stratospheric winds [*Holton*, 1983]. It is therefore possible that some of the QBO signature seen in the Saskatoon mesospheric winds is linked to the stratospheric dynamics at Saskatoon.

To investigate the possibility that the QBO signature in Saskatoon mesospheric winds might be mediated through the underlying stratosphere and to confirm that the Holton-Tan relationship holds for Saskatoon over the time period we are investigating, late winter monthly mean winds spanning pressure levels from 1 to 70 hPa derived from the ERA-Interim data set at Saskatoon were differenced with respect to the phase of the Singapore equatorial QBO at 45 hPa. The results are presented in Figure 3.9. The vertical axis shows the height in hPa and horizontal axis shows the difference between 45 hPa QBO westerly-easterly conditions in m/s. It can be seen that winds below 3 hPa in the Saskatoon stratosphere strengthen when the equatorial QBO (45 hPa) is westerly, consistent with the Holton-Tan relationship. This modulation of the late-winter stratospheric winds maximizes at 10 m/s at around 10 hPa consistent with the results of *Dunkerton and Baldwin* [1991]. We note that this relation between Saskatoon lower stratospheric winds and QBO at 45 hPa during late winter is opposite to that of the Saskatoon mesospheric winds (∼95 km) as discussed in connection with Figure 3.8.

Saskatoon- HF Radar Mesospheric Winds vs. ECMWF Stratospheric Winds: To further investigate the relationship between the mid-latitude mesosphere and stratosphere, a correlation analysis is performed between the Saskatoon HF radar mesospheric winds and the Saskatoon ECMWF stratospheric winds. Figure 3.10 shows the results. It should be noted that the HF radar mesospheric winds are obtained at a constant altitude of ∼95km, whereas the stratospheric winds derived from ECMWF span the altitudes from

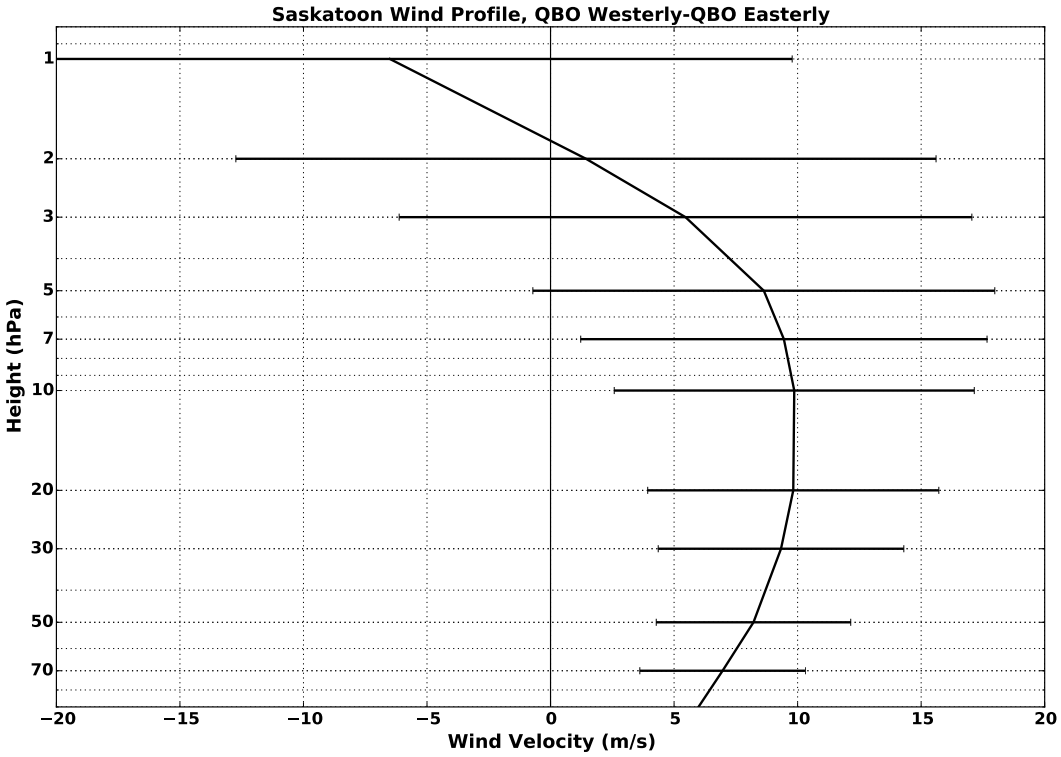

Figure 3.9: Difference between Saskatoon stratospheric zonal winds of Westerly and Easterly QBO conditions. The Saskatoon winds are derived from the ECMWF ERA-Interim data set and averaged for Jan-Feb for 2002-2014. The QBO phase is defined by the direction of the winds measured by the Singapore radiosonde at 45 hPa. The vertical axis shows the height in hPa in the Saskatoon stratosphere and horizontal axis shows the difference in wind magnitudes in m/s.

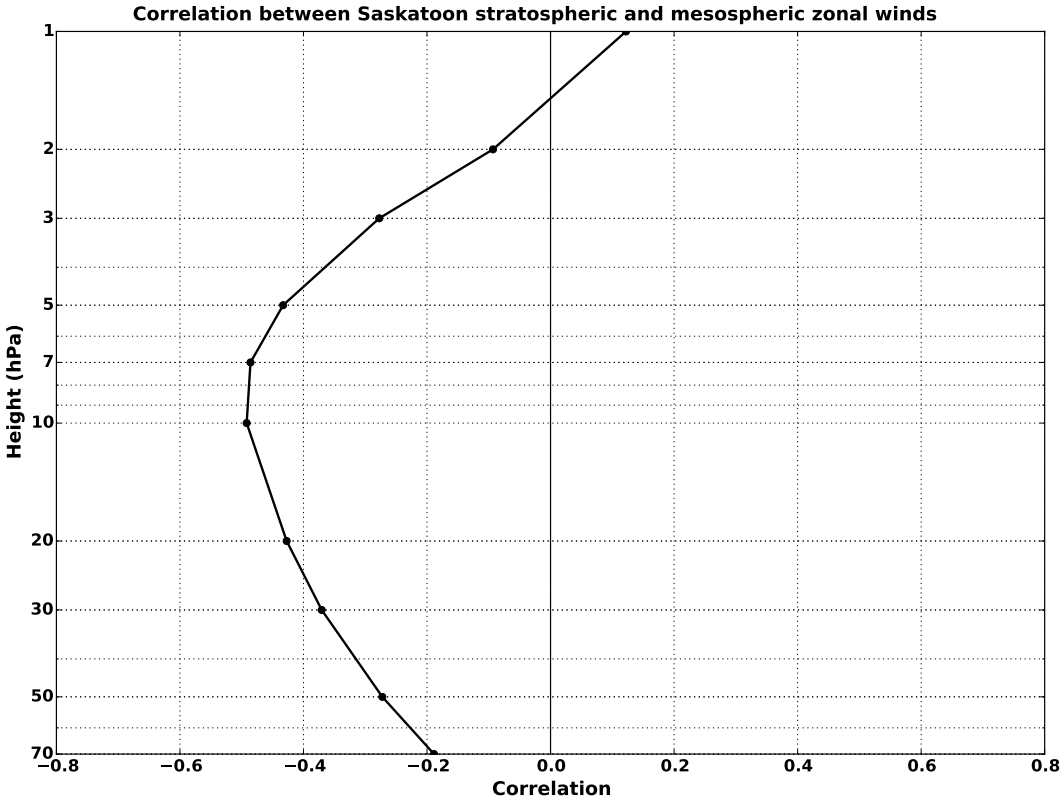

Figure 3.10: Correlation between averaged late winter (Jan-Feb) mesospheric zonal winds measured by the Saskatoon radar and zonal winds derived from ECMWF at Saskatoon at all the pressure levels identified on the left vertical axis for 2002-2014. The vertical axis shows the height in hPa and horizontal axis shows the correlation magnitudes.

1 to 70 hPa. The vertical axis shows the ECMWF wind height in hPa and horizontal axis shows the correlation magnitudes. A negative correlation below 2 hPa, maximizing to ∼-0.49 (∼91% significant) at ∼7-10 hPa, indicates that mesospheric winds are negatively correlated with the stratospheric winds at Saskatoon below 2 hPa. This negative correlation between the stratospheric and mesospheric winds at Saskatoon provides a basis for concluding that the QBO signature in Saskatoon mesospheric winds is indeed mediated through the underlying stratosphere. In the next section, we discuss a possible mechanism based on vertical coupling.

3.4 Discussion

In this study we have identified a Quasi-Biennial signature in mesospheric winds measured by the Saskatoon HF radar, that is correlated with the equatorial QBO (Figure 3.5, 3.6, 3.7). This feature is strongest during late winter (Jan-Feb) when winds in the Saskatoon mesosphere are negatively correlated with the QBO (∼45-50 hPa) such that when QBO is easterly (westerly), Saskatoon mesospheric winds tend to become more (less) westerly (Figure 3.8). By contrast, the Saskatoon ECMWF stratospheric winds become less (more) westerly during easterly (westerly) QBO (Figure 3.9). The stratospheric and mesospheric winds at Saskatoon are thus anti-correlated during late winter (Figure 3.10). In this section we discuss these results in the context of previous studies and search for a mechanism which may provide a causative explanation for the correlations we have identified linking the equatorial QBO to the Saskatoon mesospheric winds.

Previous observational and modeling studies have reported a disturbed, warmer polar vortex during the easterly phase of QBO (∼50 hPa) as opposed to a stable, colder polar vortex during its westerly phase [*Holton and Tan*, 1980, 1982; *Baldwin et al.*, 2001; *Anstey and Shepherd*, 2014]. This is sometimes referred to as the Holton-Tan (HT) effect [*Garfinkel et al.*, 2012; *Lu et al.*, 2014] after *Holton and Tan* [1980], who first explained it in terms of QBO influence on winter planetary wave activity. Previous studies have reported that the HT effect is generally felt throughout the winter, although the relationship is more robust in early winter than in late winter [*Dunkerton and Baldwin*, 1991; *Lu et al.*, 2008]. The difference climatology presented in Figure 3.9 indicates that the weakening of winter westerly winds during easterly phase of QBO, holds true for the mid-latitude Saskatoon stratosphere during January-February between 2002 and 2014 as well. How this influence becomes manifested in the Saskatoon mesosphere is the next question that needs to be considered.

Figure 3.10 shows a clear anti-correlation between Saskatoon mesospheric and stratospheric winds which could conceivably be explained by gravity wave coupling between the two regions. It is well established that as atmospheric gravity waves propagate upwards and are filtered by stratospheric zonal winds, they become unstable and deposit net wave momentum flux in the mesosphere that is in the opposite direction to the stratospheric winds [e.g.,

Fritts and Alexander, 2003]. It is possible that the QBO signature in Saskatoon mesospheric winds seen in Figure 3.8 is a result of a similar process. Namely, when the stratospheric winds at mid-latitudes are anomalously westward during easterly QBO (HT effect), the westward gravity waves are filtered out leaving an excess of eastward momentum carried into the mesosphere, causing an enhanced eastwards forcing in the mesosphere as they break and deposit their momentum. The opposite would happen when stratospheric winds are anomalously eastward during westerly QBO (i.e., the eastward gravity waves are filtered out resulting in enhanced westwards forcing in the mesosphere). Thus, the opposite phase relationship between the equatorial QBO and QBO signal seen in the mid-latitude mesosphere provides strong evidence that the QBO signal seen in the Saskatoon upper mesosphere is due to QBO modulation of the gravity wave momentum flux by the mid-latitude stratospheric winds. Such an effect is predicted by inter-hemispheric coupling mechanisms that link perturbations in the winter stratosphere to the summer hemisphere [*Karlsson et al.*, 2007, 2009; *Körnich and Becker*, 2010]. For example, *Espy et al.* [2011] have shown that a QBO signal in the high latitude summer mesopause temperatures can be coupled to the state of the winter stratosphere, the mechanism for which requires a QBO modulation of the gravity wave momentum flux in the winter hemisphere which in turn modulates the meridional pole-to-pole circulation in the mesosphere [*Murphy et al.*, 2012].

The timing of the mesospheric QBO signal varies between low and high latitudes. At the equator, QBO signature in the mesosphere is generally observed during spring equinox [*Burrage et al.*, 1996; *Garcia et al.*, 1997; *Venkateswara Rao et al.*, 2012]. The mesospheric QBO signal at high southern latitudes is observed to be present throughout the winter [*Ford et al.*, 2009] whereas the QBO signature in the Saskatoon mesosphere identified in this study is most pronounced during late winter. Thus, further modeling work is required to understand the interplay between the seasonal cycle and the global mesospheric QBO signal.

In summary, we postulate that the QBO signature we have identified in the Saskatoon late-winter mesosphere is most likely to be explained by forcing by gravity waves that have been filtered through QBO-modulated stratospheric winds. These results provide additional evidence of extratropical QBO signal at mesospheric heights, and offer supporting evidence that

the QBO perturbations to the winter stratosphere can potentially be coupled to the summer hemisphere. However, we note that long-term observations of mid-latitude mesospheric gravity wave momentum flux spanning several cycles of QBO are required to support these conclusions.

3.5 Summary and Conclusions

In this study, we have used 13 years of data (2002-2014) from the mid-latitude Saskatoon SuperDARN radar to identify a QBO signature in the Saskatoon mesospheric winds. This QBO signature in the mesospheric winds is such that, when QBO ($\sim$45 hPa) is easterly during late winter, the Saskatoon mesospheric winds become more westerly. We observed that the largest QBO effect in the Saskatoon mesosphere is observed during late winter. We also consider the Saskatoon stratospheric winds and found that when the equatorial QBO ($\sim$45 hPa) is easterly, the stratospheric winds become less westerly in agreement with previous studies and the Holton-Tan effect. This hints at vertical coupling between the two regions via gravity wave filtering. Namely, when the Saskatoon stratospheric winds are anomalously westward during easterly QBO (HT effect), the gravity waves having westward momentum are filtered out, leading to deposition of a net eastward momentum in the mesosphere. This would result in increased westerly mesospheric winds at Saskatoon. The opposite would happen when the equatorial QBO is westerly.

The QBO signal in the mid-latitude mesosphere reported here is a remarkable example of the coupling between equatorial stratosphere and mid-latitude mesosphere via meridional effects of equatorial QBO and vertically propagating gravity waves at mid-latitudes. Further studies need to be done to completely understand the dynamic effects of equatorial QBO in the mid- and high- latitude mesospheres.

This work was supported by National Science Foundation grants AGS-1341918 and AGS-1150789. Additional support is provided by the Research Council of Norway/COE under contract 223252/F50 (REH). The authors acknowledge the use of Saskatoon SuperDARN radar data. SuperDARN is a network of radars funded by national scientific funding agencies of Australia, Canada, China, France, Japan, South Africa, United Kingdom, and the United States of America. We also acknowledge the use of ECMWF ERA Interim data set from their website http://apps.ecmwf.int/datasets/data/interim-full-moda/levtype=pl/ for the Saskatoon stratospheric winds and the QBO data set provided by FU Berlin at their website http://www.geo.fu-berlin.de/en/met/ag/strat/produkte/qbo/.

Chapter 4

Summary and Future Work

4.1 Summary

In this work, we devised tools to extract meteor echoes from the backscatter obtained by HF SuperDARN radars in the near-range gates. Then, we developed new techniques to calculate the zonal and meridional components of the neutral winds from the meteor scatter, at an altitude of ∼95 km. This dataset was then analyzed to study inter-annual variations in the mean zonal winds at the mid-latitude Saskatoon SuperDARN radar. A biennial periodicity was found in the late winter mesospheric mean zonal winds. We compared this feature with the Quasi Biennial Oscillation in the equatorial stratosphere and found that they are negatively correlated such that when the QBO at 45 hPa at the equator is easterly, the Saskatoon late winter mesospheric winds become more westerly, whereas when QBO is westerly, the Saskatoon winds become less westerly (decrease in magnitude). In order to find the link between equatorial stratosphere and mid-latitude mesosphere, we also studied the Saskatoon stratospheric winds and found that they become less westerly when QBO is in easterly phase and more westerly when QBO is in the westerly phase. Thus, we conclude that the effect of QBO on mid-latitude stratospheric winds is essentially the same as that on the high-latitude polar vortex (Holton-Tan effect) and gravity wave filtering through the QBO-modulated stratospheric winds and opposite momentum deposition in MLT is the

source of QBO signal in Saskatoon mesosphere. However, the reason, why this signal appears strongest only in late winter, is still not understood.

4.2 Future Work

This section aims to introduce two main ideas that need further investigation to understand the dynamical coupling of QBO with extratropical mesosphere. In our analysis, we find that apart from late winter (as presented in Chapter 3), the mesospheric QBO signature at Saskatoon is also significant in August and thus deserves further investigation. We also discuss the longitudinal variability in the extratropical influence of QBO.

4.2.1 QBO signal in August

As seen in Figure 3.6, apart from late winter, the winds in the Saskatoon mesosphere show a significant correlation with the QBO (30-50 hPa) in August. From Figure 3.7, the difference between the two QBO climatologies (if QBO phase is defined by the direction of winds at 45-50 hPa above the equator), is $\sim$ 2-3 m/s. This difference in the winds is marginal compared to the magnitude in Jan-Feb (dark blue and red patches on the left of Figure 3.7), however, it is still significant. The mechanism that would result in this QBO signal in late summer mesosphere is unknown, and not many studies have acknowledged its presence owing to its low magnitude.

Due to the significant difference between the westerly and easterly QBO climatologies of the Saskatoon stratosphere (in Jan-Feb) in Figure 3.9, we concluded in the previous chapter that the QBO signal in the Saskatoon stratosphere is carried over into the mesosphere via gravity waves. We plot the same data for the stratosphere at Saskatoon during August to find the source of mesospheric QBO signal during this time. The result is shown in Figure 4.1. This figure clearly shows that there is almost no influence of QBO phases on the stratospheric winds during August, and hence the mechanism should be different than that observed in late winter. Thus, further investigation into the source of August mesospheric QBO signal,

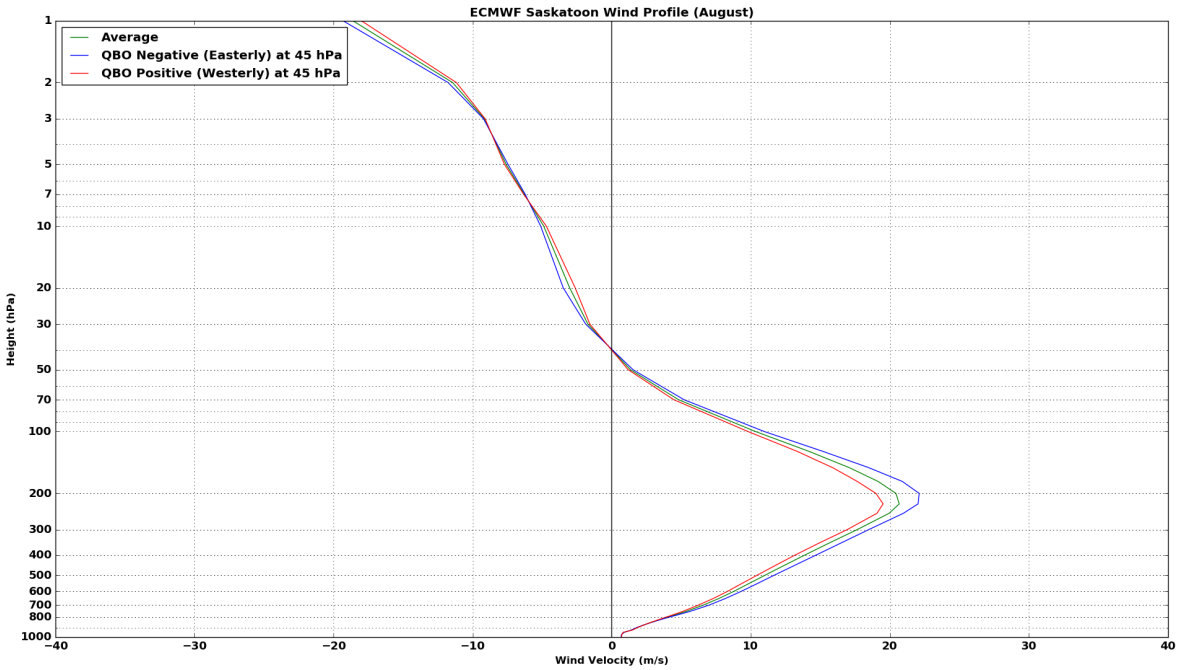

Figure 4.1: Saskatoon wind profile averaged for August (2002-2014), separated by the phase of QBO at 45 hPa. Green represents the average climatology, Red represents when QBO is westerly and Blue represents when QBO is in easterly phase. The horizontal axis represents wind velocity in m/s and the vertical axis represents height in hPa in the Saskatoon stratosphere.

is crucial to completely understand the effects of QBO in extratropical stratosphere and mesosphere, and the mechanism involved.

4.2.2 QBO climatologies for Other Radars

Figure 4.2 shows the mesospheric wind climatologies of three SuperDARN radars, (from top to bottom) PGR (53.98°N, -122.59°E), KAP (49.39°N, -82.32°E) and GBR (53.32°N, -60.46°E). These climatologies are separated into phases of QBO. We can observe the longitudinal differences in the effect of QBO in different seasons. Thus, the extratropical effects of QBO are not uniform in longitude, for example, the difference between red and blue curves

is larger in Jan-Feb at KAP, and much smaller at PGR and GBR. These differences further indicate the possible link between QBO signal and planetary waves (as planetary waves have a zonal wavenumber associated with them). This study will especially benefit from the location of SuperDARN radars at mid and high latitudes (at about the same latitude circle), and will greatly improve our understanding of the mechanism of coupling between the equatorial stratosphere and extratropical latitudes via planetary waves.

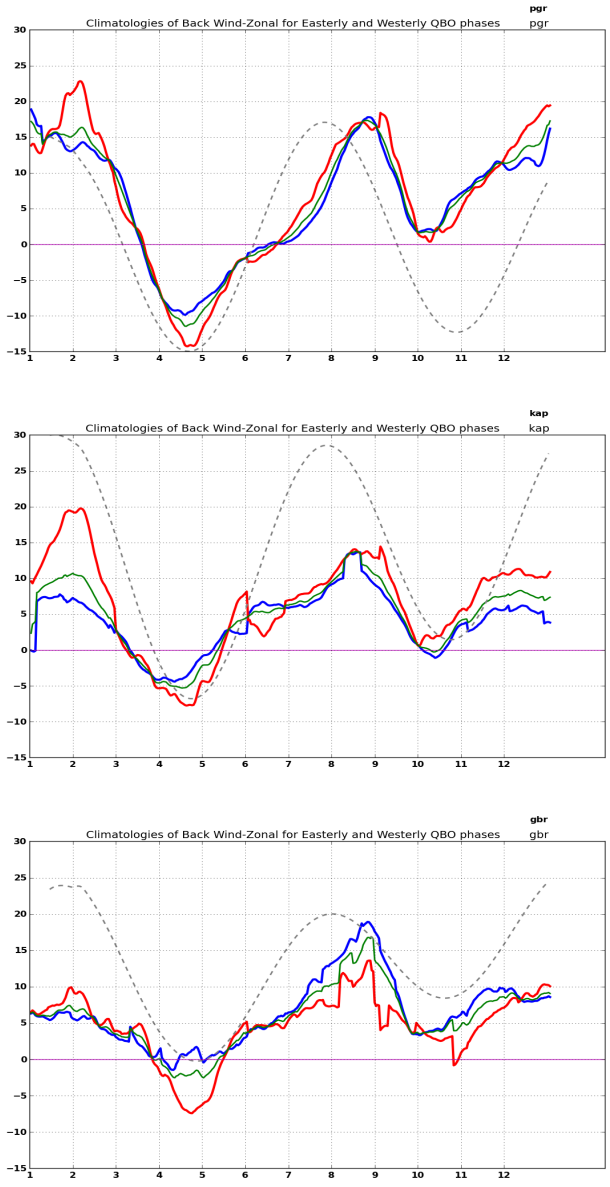

Figure 4.2: QBO climatologies for mid latitude SuperDARN radars, PGR (53.98°N, -122.59°E), KAP (49.39°N, -82.32°E) and GBR (53.32°N, -60.46°E). The panels show the Mean Zonal Background Wind Climatology (30-day Rolling Mean) at different radars averaged between 2007-2014 (Green) along with the climatologies during QBO easterly (Red) and westerly (Blue) phase, as defined at 50 hPa at the equator, Gray dotted line shows HWM model averaged between 85-95 km. For all the panels, the horizontal axes represent the month of the year and the vertical axes represent wind velocities in m/s.

Bibliography

Andrews, D. G., J. R. Holton, and C. B. Leovy (1987), *Middle atmosphere dynamics.*, Academic Press, New York, NY, USA. 489.

Anstey, J. A., and T. G. Shepherd (2014), High-latitude influence of the quasi-biennial oscillation, *Quarterly Journal of the Royal Meteorological Society*, *140*(678), 1–21, doi: 10.1002/qj.2132.

Baldwin, M. P., and T. J. Dunkerton (1998), Quasi-biennial modulation of the southern hemisphere stratospheric polar vortex, *Geophysical Research Letters*, *25*(17), 3343–3346, doi:10.1029/98GL02445.

Baldwin, M. P., L. J. Gray, T. J. Dunkerton, K. Hamilton, P. H. Haynes, W. J. Randel, J. R. Holton, M. J. Alexander, I. Hirota, T. Horinouchi, D. B. A. Jones, J. S. Kinnersley, C. Marquardt, K. Sato, and M. Takahashi (2001), The quasi-biennial oscillation, *Reviews of Geophysics*, *39*(2), 179–229, doi:10.1029/1999RG000073.

Baumgaertner, A., A. McDonald, G. Fraser, and G. Plank (2005), Long-term observations of mean winds and tides in the upper mesosphere and lower thermosphere above Scott base, Antarctica, *Journal of Atmospheric and Solar-Terrestrial Physics*, *67*(16), 1480 – 1496, doi:http://dx.doi.org/10.1016/j.jastp.2005.07.018.

Belmont, A. D., and D. G. Dartt (1968), Variation with longitude of the Quasi-Biennial Oscillation, *Mon. Weather Rev.*, *96*, 767–777.

Belmont, A. D., and G. D. Nastrom (1979), Long-period waves in mesospheric winds at Saskatoon (52°N), *Journal of Geomagnetism and Geoelectricity*, *31*, 165–171.

Berrisford, P., D. Dee, K. Fielding, M. Fuentes, P. Kallberg, S. Kobayashi, and S. Uppala (2009), The Era-Interim Archive, *ERA Report Series,No.1. ECMWF: Reading, UK.*

Bristow, W. A., J.-H. Yee, X. Zhu, and R. A. Greenwald (1999), Simultaneous observations of the July 1996 2-day wave event using the Super Dual Auroral Radar Network and the High Resolution Doppler Imager, *Journal of Geophysical Research: Space Physics*, *104*(A6), 12,715–12,721, doi:10.1029/1999JA900030.

Burrage, M. D., R. A. Vincent, H. G. Mayr, W. R. Skinner, N. F. Arnold, and P. B. Hays (1996), Long-term variability in the equatorial middle atmosphere zonal wind, *Journal of Geophysical Research: Atmospheres*, *101*(D8), 12,847–12,854, doi:10.1029/96JD00575.

Chisham, G., et al. (2007), A decade of the Super Dual Auroral Radar Network (SuperDARN): Scientific achievements, new techniques and future directions, *Surv. Geophys.*, *28*, 33–109, doi:10.1007/a10712-007-9017-8.

de Wit, R. J., R. E. Hibbins, P. J. Espy, and N. J. Mitchell (2013), Interannual variability of mesopause zonal winds over Ascension Island: Coupling to the stratospheric QBO, *Journal of Geophysical Research: Atmospheres*, *118*(21), 12,052–12,060, doi: 10.1002/2013JD020203.

Dee, D. P., S. M. Uppala, A. J. Simmons, P. Berrisford, P. Poli, S. Kobayashi, U. Andrae, M. A. Balmaseda, G. Balsamo, P. Bauer, P. Bechtold, A. C. M. Beljaars, L. van de Berg, J. Bidlot, N. Bormann, C. Delsol, R. Dragani, M. Fuentes, A. J. Geer, L. Haimberger, S. B. Healy, H. Hersbach, E. V. Hlm, L. Isaksen, P. Kllberg, M. Khler, M. Matricardi, A. P. McNally, B. M. Monge-Sanz, J.-J. Morcrette, B.-K. Park, C. Peubey, P. de Rosnay, C. Tavolato, J.-N. Thpaut, and F. Vitart (2011), The ERA-interim reanalysis: configuration and performance of the data assimilation system, *Quarterly Journal of the Royal Meteorological Society*, *137*(656), 553–597, doi:10.1002/qj.828.

Dunkerton, T. J. (1997), The role of gravity waves in the quasi-biennial oscillation, *Journal of Geophysical Research: Atmospheres*, *102*(D22), 26,053–26,076, doi:10.1029/96JD02999.

Dunkerton, T. J., and M. P. Baldwin (1991), Quasi-biennial modulation of planetary-wave fluxes in the northern hemisphere winter, *Journal of the Atmospheric Sciences*, *48*(8), 1043–1061.

Ebdon, R. A. (1960), Notes on the wind flow at 50 mb in tropical and sub-tropical regions in January 1957 and January 1958, *Quarterly Journal of the Royal Meteorological Society*, *86*(370), 540–542, doi:10.1002/qj.49708637011.

Espy, P. J., J. Stegman, and G. Witt (1997), Interannual variations of the quasi-16-day oscillation in the polar summer mesospheric temperature, *Journal of Geophysical Research: Atmospheres*, *102*(D2), 1983–1990, doi:10.1029/96JD02717.

Espy, P. J., R. E. Hibbins, D. M. Riggin, and D. C. Fritts (2005), Mesospheric planetary waves over Antarctica during 2002, *Geophysical Research Letters*, *32*(21), doi:10.1029/2005GL023886, l21804.

Espy, P. J., S. Ochoa Fernández, P. Forkman, D. Murtagh, and J. Stegman (2011), The role of the QBO in the inter-hemispheric coupling of summer mesospheric temperatures, *Atmospheric Chemistry and Physics*, *11*(2), 495–502, doi:10.5194/acp-11-495-2011.

Ford, E. A. K., R. E. Hibbins, and M. J. Jarvis (2009), QBO effects on Antarctic mesospheric winds and polar vortex dynamics, *Geophysical Research Letters*, *36*(20), doi:10.1029/2009GL039848, l20801.

Fritts, D. C., and M. J. Alexander (2003), Gravity wave dynamics and effects in the middle atmosphere, *Reviews of Geophysics*, *41*(1), doi:10.1029/2001RG000106, 1003.

Garcia, R. R., T. J. Dunkerton, R. S. Lieberman, and R. A. Vincent (1997), Climatology of the semiannual oscillation of the tropical middle atmosphere, *Journal of Geophysical Research: Atmospheres*, *102*(D22), 26,019–26,032, doi:10.1029/97JD00207.

Garfinkel, C. I., T. A. Shaw, D. L. Hartmann, and D. W. Waugh (2012), Does the Holton-Tan Mechanism Explain How the Quasi-Biennial Oscillation Modulates the Arctic Polar Vortex?, *Journal of the Atmospheric Sciences*, *69*(5), 1713–1733, doi:10.1175/JAS-D-11-0209.1.

Gray, L. J., S. J. Phipps, T. J. Dunkerton, M. P. Baldwin, E. F. Drysdale, and M. R. Allen (2001a), A data study of the influence of the equatorial upper stratosphere on northern-hemisphere stratospheric sudden warmings, *Quarterly Journal of the Royal Meteorological Society*, *127*(576), 1985–2003, doi:10.1002/qj.49712757607.

Gray, L. J., E. F. Drysdale, B. N. Lawrence, and T. J. Dunkerton (2001b), Model studies of the interannual variability of the northern-hemisphere stratospheric winter circulation: The role of the quasi-biennial oscillation, *Quarterly Journal of the Royal Meteorological Society*, *127*(574), 1413–1432, doi:10.1002/qj.49712757416.

Gray, L. J., S. Crooks, C. Pascoe, S. Sparrow, and M. Palmer (2004), Solar and QBO Influences on the Timing of Stratospheric Sudden Warmings, *Journal of the Atmospheric Sciences*, *61*(23), 2777–2796, doi:10.1175/JAS-3297.1.

Greenwald, R. A., K. B. Baker, R. A. Hutchins, and C. Hanuise (1985), An HF phased-array radar for studying small-scale structure in the high-latitude ionosphere, *Radio Science*, *20*(1), 63–79, doi:10.1029/RS020i001p00063.

Groves, G. V. (1973), Zonal wind quasi-biennial oscillations at 25-60 km altitude, 1962-69, *Quarterly Journal of the Royal Meteorological Society*, *99*(419), 73–81, doi:10.1002/qj.49709941907.

Hall, G. E., J. W. MacDougall, D. R. Moorcroft, J.-P. St.-Maurice, A. H. Manson, and C. E. Meek (1997), Super Dual Auroral Radar Network observations of meteor echoes, *Journal of Geophysical Research: Space Physics*, *102*(A7), 14,603–14,614, doi:10.1029/97JA00517.

Hibbins, R., O. Marsh, A. McDonald, and M. Jarvis (2010), Interannual variability of the S=1 and S=2 components of the semidiurnal tide in the Antarctic MLT, *Journal of Atmospheric and Solar-Terrestrial Physics*, *72*(910), 794 – 800, doi:http://dx.doi.org/10.1016/j.jastp.2010.03.026.

Hibbins, R. E., and M. J. Jarvis (2008), A long-term comparison of wind and tide measurements in the upper mesosphere recorded with an imaging Doppler interferometer and

SuperDARN radar at Halley, Antarctica, *Atmospheric Chemistry and Physics*, *8*(5), 1367–1376, doi:10.5194/acp-8-1367-2008.

Hibbins, R. E., P. J. Espy, and M. J. Jarvis (2007), Quasi-biennial modulation of the semidiurnal tide in the upper mesosphere above Halley, Antarctica, *Geophysical Research Letters*, *34*(21), doi:10.1029/2007GL031282, l21804.

Hibbins, R. E., M. J. Jarvis, and E. A. K. Ford (2009), Quasi-biennial oscillation influence on long-period planetary waves in the Antarctic upper mesosphere, *Journal of Geophysical Research: Atmospheres*, *114*(D9), doi:10.1029/2008JD011174, d09109.

Holton, J. R. (1983), The influence of gravity wave breaking on the General Circulation of the Middle Atmosphere, *Journal of the Atmospheric Sciences*, *40*(10), 2497–2507.

Holton, J. R., and R. S. Lindzen (1972), An updated theory for the Quasi-Biennial Cycle of the Tropical Stratosphere, *Journal of the Atmospheric Sciences*, *29*(6), 1076–1080.

Holton, J. R., and H.-C. Tan (1980), The Influence of the Equatorial Quasi-Biennial Oscillation on the Global Circulation at 50 mb, *Journal of the Atmospheric Sciences*, *37*(10), 2200–2208.

Holton, J. R., and H.-C. Tan (1982), The Quasi-Biennial Oscillation in the northern hemisphere lower stratosphere, *Journal of the Meteorological Society of Japan. Ser. II*, *60*(1), 140–148.

Hussey, G. C., C. E. Meek, D. Andr, A. H. Manson, G. J. Sofko, and C. M. Hall (2000), A comparison of northern hemisphere winds using SuperDARN meteor trail and MF radar wind measurements, *Journal of Geophysical Research: Atmospheres*, *105*(D14), 18,053–18,066, doi:10.1029/2000JD900272.

Jarvis, M. J. (1996), Quasi-Biennial Oscillation effects in the semidiurnal tide of the Antarctic lower thermosphere, *Geophysical Research Letters*, *23*(19), 2661–2664, doi:10.1029/96GL02394.

Jenkins, B., and M. Jarvis (1999), Mesospheric winds derived from SuperDARN HF radar meteor echoes at Halley, Antarctica, *Earth, Planets and Space*, *51*(7-8), 685–689, doi: 10.1186/BF03353226.

Jenkins, B., M. J. Jarvis, and D. M. Forbes (1998), Mesospheric wind observations derived from Super Dual Auroral Radar Network (SuperDARN) HF radar meteor echoes at Halley, Antarctica: Preliminary results, *Radio Science*, *33*(4), 957–965, doi:10.1029/98RS01113.

Johnson, R. M., and T. L. Killeen (1995), *The Upper Mesosphere and Lower Thermosphere: A Review of Experiment and Theory*, vol. 87, 23–36 pp., Geophysical Monograph 87.

Kane, R. P., C. E. Meek, and A. H. Manson (1999), Quasi-biennial and higher-period oscillations in the mean winds in the mesosphere and lower thermosphere over Saskatoon, 52°N, 107°W, *Journal of Geophysical Research: Space Physics*, *104*(A2), 2645–2652, doi: 10.1029/1998JA900066.

Karlsson, B., H. Körnich, and J. Gumbel (2007), Evidence for interhemispheric stratosphere-mesosphere coupling derived from noctilucent cloud properties, *Geophysical Research Letters*, *34*(16), doi:10.1029/2007GL030282, l16806.

Karlsson, B., C. McLandress, and T. G. Shepherd (2009), Inter-hemispheric mesospheric coupling in a comprehensive middle atmosphere model, *Journal of Atmospheric and Solar-Terrestrial Physics*, *71*(34), 518 – 530, doi:http://dx.doi.org/10.1016/j.jastp.2008.08.006.

Kawatani, Y., and K. Hamilton (2013), Weakened stratospheric quasibiennial oscillation driven by increased tropical mean upwelling, *Nature*, *497*(7450), 478–481, letter.

Kelley, M. C. (2009), *The Earth's Ionosphere, Plasma Physics and Electrodynamics*, vol. 96, second ed., 20–22 pp., Academic Press.

Kleinknecht, N. H., P. J. Espy, and R. E. Hibbins (2014a), The climatology of zonal wave numbers 1 and 2 planetary wave structure in the MLT using a chain of northern hemisphere superdarn radars, *Journal of Geophysical Research: Atmospheres*, *119*(3), 1292–1307, doi: 10.1002/2013JD019850.

Kleinknecht, N. H., P. J. Espy, and R. E. Hibbins (2014b), The climatology of zonal wave numbers 1 and 2 planetary wave structure in the MLT using a chain of Northern Hemisphere SuperDARN radars, *Journal of Geophysical Research: Atmospheres*, *119*(3), 1292–1307, doi:10.1002/2013JD019850.

Körnich, H., and E. Becker (2010), A simple model for the interhemispheric coupling of the middle atmosphere circulation, *Advances in Space Research*, *45*(5), 661 – 668, doi:http://dx.doi.org/10.1016/j.asr.2009.11.001.

Kürschner, D., and C. Jacobi (2003), Quasi-biennial and decadal variability obtained from long-term measurements of nighttime radio wave reflection heights over Central Europe, *Advances in Space Research*, *32*(9), 1701 – 1706, doi:http://dx.doi.org/10.1016/S0273-1177(03)90465-0.

Labitzke, K., and H. V. Loon (1988), Associations between the 11-year solar cycle, the QBO and the atmosphere. Part I: the troposphere and stratosphere in the northern hemisphere in winter, *Journal of Atmospheric and Terrestrial Physics*, *50*(3), 197 – 206, doi:http://dx.doi.org/10.1016/0021-9169(88)90068-2.

Lindzen, R. S., and J. R. Holton (1968), A Theory of the Quasi-Biennial Oscillation, *Journal of the Atmospheric Sciences*, *25*(6), 1095–1107.

Lu, H., M. P. Baldwin, L. J. Gray, and M. J. Jarvis (2008), Decadal-scale changes in the effect of the QBO on the northern stratospheric polar vortex, *Journal of Geophysical Research: Atmospheres*, *113*(D10), doi:10.1029/2007JD009647, d10114.

Lu, H., L. J. Gray, M. P. Baldwin, and M. J. Jarvis (2009), Life cycle of the QBO-modulated 11-year solar cycle signals in the Northern Hemispheric winter, *Quarterly Journal of the Royal Meteorological Society*, *135*(641), 1030–1043, doi:10.1002/qj.419.

Lu, H., T. J. Bracegirdle, T. Phillips, A. Bushell, and L. Gray (2014), Mechanisms for the Holton-Tan relationship and its decadal variation, *Journal of Geophysical Research: Atmospheres*, *119*(6), 2811–2830, doi:10.1002/2013JD021352.

Malinga, S. B., and J. M. Ruohoniemi (2007), The quasi-two-day wave studied using the Northern Hemisphere SuperDARN HF radars, *Annales Geophysicae*, *25*(8), 1767–1778, doi:10.5194/angeo-25-1767-2007.

Manson, A., and C. Meek (1986), Dynamics of the middle atmosphere at Saskatoon (52°N, 107°W): a spectral study during 1981, 1982, *Journal of Atmospheric and Terrestrial Physics*, *48*(1112), 1039 – 1055, doi:http://dx.doi.org/10.1016/0021-9169(86)90025-5.

Manson, A. H., C. E. Meek, and J. B. Gregory (1981), Long-Period oscillations in mesospheric and lower thermospheric winds (60-110km) at Saskatoon (52°N, 107°W, L=4.3), *Journal of geomagnetism and geoelectricity*, *33*(12), 613–621, doi:10.5636/jgg.33.613.

Matthews, D., M. Parkinson, P. Dyson, and J. Devlin (2006), Optimising estimates of mesospheric neutral wind using the TIGER Superdarn radar, *Advances in Space Research*, *38*(11), 2353 – 2360, doi:http://dx.doi.org/10.1016/j.asr.2005.07.046.

Mayr, H. G., J. G. Mengel, C. O. Hines, K. L. Chan, N. F. Arnold, C. A. Reddy, and H. S. Porter (1997), The gravity wave Doppler spread theory applied in a numerical spectral model of the middle atmosphere: 1. Model and global scale seasonal variations, *Journal of Geophysical Research: Atmospheres*, *102*(D22), 26,077–26,091, doi:10.1029/96JD03213.

Mayr, H. G., J. G. Mengel, and F. T. Huang (2009), Modeling the temperature of the polar mesopause region: Part I- Inter-annual and long-term variations generated by the stratospheric QBO, *Journal of Atmospheric and Solar-Terrestrial Physics*, *71*(34), 497 – 507, doi:http://dx.doi.org/10.1016/j.jastp.2008.09.033.

Middleton, H. R., N. J. Mitchell, and H. G. Muller (2002), Mean winds of the mesosphere and lower thermosphere at 52°N in the period 1988-2000, *Annales Geophysicae*, *20*(1), 81–91, doi:10.5194/angeo-20-81-2002.

Murphy, D. J., S. P. Alexander, and R. A. Vincent (2012), Interhemispheric dynamical coupling to the southern mesosphere and lower thermosphere, *Journal of Geophysical Research: Atmospheres*, *117*(D8), doi:10.1029/2011JD016865, d08114.

Naito, Y., and I. Hirota (1997), Interannual variability of the northern winter stratospheric circulation related to the QBO and the solar cycle, *J. Meteor. Soc. Japan*, *75*, 925–937.

Namboothiri, S., A. Manson, and C. Meek (1993), Variations of mean winds and tides in the upper middle atmosphere over a solar cycle, Saskatoon, Canada, 52°N, 107°W, *Journal of Atmospheric and Terrestrial Physics*, *55*(10), 1325 – 1334, doi:http://dx.doi.org/10.1016/0021-9169(93)90101-4.

Namboothiri, S., C. Meek, and A. Manson (1994), Variations of mean winds and solar tides in the mesosphere and lower thermosphere over time scales ranging from 6 months to 11 yr: Saskatoon, 52°N, 107°W, *Journal of Atmospheric and Terrestrial Physics*, *56*(10), 1313 – 1325, doi:http://dx.doi.org/10.1016/0021-9169(94)90069-8.

Naoe, H., and K. Shibata (2010), Equatorial quasi-biennial oscillation influence on northern winter extratropical circulation, *Journal of Geophysical Research: Atmospheres*, *115*(D19), doi:10.1029/2009JD012952, d19102.

Naujokat, B. (1986), An Update of the Observed Quasi-Biennial Oscillation of the Stratospheric Winds over the Tropics., *Journal of Atmospheric Sciences*, *43*, 1873–1880.

Neumann, A. (1990), QBO and solar activity effects on temperatures in the mesopause region, *Journal of Atmospheric and Terrestrial Physics*, *52*(3), 165 – 173, doi:http://dx.doi.org/10.1016/0021-9169(90)90120-C.

Ogawa, T., N. Nishitani, N. Sato, H. Yamagishi, and A. S. Yukimatu (2002), Upper mesosphere summer echoes detected with the antarctic syowa hf radar, *Geophysical Research Letters*, *29*(7), 61–1–61–4, doi:10.1029/2001GL014094.

Ogawa, T., S. Nozawa, M. Tsutsumi, N. F. Arnold, N. Nishitani, N. Sato, and A. S. Yukimatu (2004), Arctic and Antarctic polar mesosphere summer echoes observed with oblique incidence HF radars: analysis using simultaneous MF and VHF radar data, *Annales Geophysicae*, *22*(12), 4049–4059, doi:10.5194/angeo-22-4049-2004.

Pascoe, C. L., L. J. Gray, and A. A. Scaife (2006), A GCM study of the influence of equatorial winds on the timing of sudden stratospheric warmings, *Geophysical Research Letters*, *33*(6), doi:10.1029/2005GL024715, l06825.

Plumb, R. A., and R. C. Bell (1982), Equatorial waves in steady zonal shear flow, *Quarterly Journal of the Royal Meteorological Society*, *108*(456), 313–334, doi:10.1002/qj.49710845603.

Portnyagin, Y. I., and T. V. Solovjova (2000), Global empirical wind model for the upper mesosphere/lower thermosphere. I. Prevailing wind, *Annales Geophysicae*, *18*(3), 300–315, doi:10.1007/s00585-000-0300-y.

Press, W. H., B. P. Flannery, S. A. Teukolsky, and W. T. Vetterling (1992), Numerical Recipes in C: The Art of Scientific Computing, 2nd edn., *Cambridge University Press, New York*.

Reed, R. J. (1965), The Quasi-Biennial Oscillation of the Atmosphere Between 30 and 50 km Over Ascension Island, *Journal of the Atmospheric Sciences*, *22*(3), 331–333.

Reed, R. J., W. J. Campbell, L. A. Rasmussen, and D. G. Rogers (1961), Evidence of a downward-propagating, annual wind reversal in the equatorial stratosphere, *Journal of Geophysical Research*, *66*(3), 813–818, doi:10.1029/JZ066i003p00813.

Ruohoniemi, J. M., R. A. Greenwald, K. B. Baker, J. P. Villain, and M. A. McCready (1987), Drift motions of small-scale irregularities in the high-latitude f region: An experimental comparison with plasma drift motions, *Journal of Geophysical Research: Space Physics*, *92*(A5), 4553–4564, doi:10.1029/JA092iA05p04553.

Sprenger, K., and R. Schminder (1968), On the significance of ionospheric drift measurements in the LF range, *Journal of Atmospheric and Terrestrial Physics*, *30*(5), 693 – 700, doi: http://dx.doi.org/10.1016/S0021-9169(68)80025-X.

Sprenger, K., K. Greisiger, and R. Schminder (1975), Evidence of quasi-biennial wind oscillation in the mid-latitude lower thermosphere, obtained from ionospheric drift measurements

in the LF range, *Journal of Atmospheric and Terrestrial Physics*, *37*(10), 1391 – 1393, doi:http://dx.doi.org/10.1016/0021-9169(75)90134-8.

Venkateswara Rao, N., T. Tsuda, D. M. Riggin, S. Gurubaran, I. M. Reid, and R. A. Vincent (2012), Long-term variability of mean winds in the mesosphere and lower thermosphere at low latitudes, *Journal of Geophysical Research: Space Physics*, *117*(A10), doi:10.1029/2012JA017850, a10312.

Wallace, J. M. (1973), General circulation of the tropical lower stratosphere, *Reviews of Geophysics*, *11*(2), 191–222, doi:10.1029/RG011i002p00191.

Xu, J., A. K. Smith, H.-L. Liu, W. Yuan, Q. Wu, G. Jiang, M. G. Mlynczak, J. M. Russell, and S. J. Franke (2009), Seasonal and quasi-biennial variations in the migrating diurnal tide observed by Thermosphere, Ionosphere, Mesosphere, Energetics and Dynamics (TIMED), *Journal of Geophysical Research: Atmospheres*, *114*(D13), doi:10.1029/2008JD011298, d13107.